Progress in Polymer Science 122 (2021) 101449

Contents lists available at ScienceDirect

Progress in Polymer Science

journal homepage: www.elsevier.com/locate/progpolymsci

Organic batteries based on just redox polymers

Nicolas Goujon [a], Nerea Casado [a], Nagaraj Patil [b], Rebeca Marcilla [b], David Mecerreyes [a,c,*]

[a] POLYMAT University of the Basque Country UPV/EHU, Avenida Tolosa 72, 20018 Donostia-San Sebastián, Spain
[b] Electrochemical Processes Unit, IMDEA Energy, Avda. Ramón de la Sagra 3, 28935 Móstoles, Madrid, Spain
[c] Ikerbasque, Basque Foundation for Science, Maria Diaz de Haro 3, E–48011 Bilbao, Spain

ARTICLE INFO

Article history:
Received 18 January 2021
Revised 27 April 2021
Accepted 27 August 2021
Available online 5 September 2021

Keywords:
Redox polymer
Organic battery
Polymers for batteries
Redox flow battery
Electroactive polymers

ABSTRACT

Redox-active polymers have gained interest as environmentally friendly alternative to inorganic materials in applications such as electrodes in lithium-ion batteries. All-polymer batteries were first disregarded with respect to other technologies due to their lower energy densities. However, the inherent benefits of redox polymers such as processability, flexibility, recyclability, high-rate performance and the perspective to prepare batteries from renewable resources has re-ignited interest in recent years. This review article aims to provide a comprehensive overview on the state of the art of batteries in which the active material is a redox polymer; including "static" all-polymer batteries and polymer-air batteries but also "flowing" systems such as polymer based redox-flow batteries (pRFB). First, a succinct overview of the recent developments of redox polymers will be given, summarizing the historic trends and developments. Second, an exhaustive discussion of the various battery prototypes will be provided, considering all steps in the development of organic batteries just based in redox polymers. Finally, future perspectives on all-polymer batteries will be discussed, summarizing the major challenges that are still to be overcome to unlock their commercial implementation.

1. Introduction

Electromobility and energy storage for renewable energy production are the main drives for the actual interest in Electrochemical Energy Storage (EES). Among the different technologies, lithium-ion batteries (LIBs) are nowadays widely used and their pioneers received the Nobel Prize in 2019. However, the current inorganic active materials, which are used as electrodes in LIBs, are showing some drawbacks and limitations. First, inorganic electrodes are reaching their theoretical capabilities (< 250 mAh/g) and second, they are based on scarce and/or toxic metals (Li, Co, Mn, Ni) with a limited or localized resource distributions [1,2]. For these reasons, organic electrode materials have been gaining a lot of interest as an environmentally friendly alternative [3,4]. The implementation of organic materials (i.e. small organic molecules and redox polymers) as elec-

Abbreviations: ACN, Acetonitrile; BODIPY, Difluoro{2-[(3,5-dimethyl-2H-pyrrol-2-ylidene-N)phenylmethyl]-3,5-dimethyl-1H-pyrrolato-N}boron; CNTs, Carbon nanotubes; CPRs, Conducting redox polymers; DHT, 3,4-dihexylthiophene; DMC, Dimethyl carbonate; DME, 1,2-dimethoxyethane; DOL, 1,3-dioxolane; EC, Ethylene carbonate; EES, Electrochemical energy storage; EMC, Ethyl methyl carbonate; EMImTFSI, 1-ethyl-3-methylimidazolium bis(trifluoromethylsulfonyl)imide; LIBs, Lithium-ion batteries; LiTFSI, Lithium bis(trifluoromethanesulfonyl)imide salt; MA, Methyl acetate; MnO2/C, Manganese dioxide/carbon; NDC, Nitrogen-doped carbon; PAN, Polyacrylonitrile; PANI, Poly(aniline); PAQE, Poly(anthraquinone-substituted ethyleneimine); PAQS, Poly(anthraquinonyl sulphide); PBPy, Poly(N-vinylcarbazole); PC, Propylene carbonate; PDB, Poly(2,3-dithiino-1,4-benzoquinone); PDHT, Poly(3,4-dihexylthiophene); PEDOT, Poly(3,4-ethylenedioxythiophene); PEDOT-AQ, Poly((2,3-dihydrothieno[3,4-b][1,4]dioxin-2-yl)methyl 9,10-dioxo-9,10-dihydroanthracene-2-carboxylate); PEDOT-BQ, Poly ((2,3-dihydrothieno[3,4-b][1,4]dioxin-2-yl)methyl 3-(2,5-dihydroxyphenyl)propanoate); PEGMA, Poly(ethylene glycol) methacrylate; PEO, Poly(ethylene oxide); pEP(NQ)E, Poly(naphthoquinone-subtitued 3,4-ethylenedioxythiophene); PI, Poly(1,4,5,8-naphthalenetetracarboxylic bisimide-1,2-para-phenyl); PI-5, Poly(1,4,5,8-naphthalenetetracarboxylic bisimide); PNB-g-PTMA, Poly(norbornene)-graft-poly(4-methacryloyloxy-2,2,6,6-tetramethylpiperidin-1-oxyl); PNQ, Poly(naphthoquinone-substituted allyamine); poly(catechol), Poly(dopamine acrylamide-r-2-acrylamido-2-methylpropane sulfonic acid); poly(imide), Poly(1,4,5,8-naphthalenetetracarboxylicdiimide-1,2-diethoxyethane); PPP, Poly(para-phenylene); pPy-V2+-Me, Poly(1-methyl-1′-(6-pyrrol-1-yl)hexyl)-4, 4′-bipyridinum); PQNB, Poly(dianthraquinone-substituted norbornene); pRFB, Polymer redox-flow batteries; PTAm, Poly(2,2,6,6-tetramethylpiperidinyloxyl-4-acrylamide); PTMA, Poly(2,2,6,6-tetramethylpiperidine-N-oxyl)methacrylate; PTPAn, Poly(triphenylamine); PTPM, Poly(tripyridiniomesitylene); PV10, Poly(N-4–4′-bipyridinium-N-decametylene dibromide); PVAQ, Poly(vinylanthraquinone); SHE, Standard hydrogen electrode; SWCNTs, Single-walled carbon nanotubes; TCAQ, 11,11,12,12-tetracyano-9,10-anthraquinonedimethane; TEMPO, 2,2,6,6-tetramethylpiperidine-1-oxyl radical; VGCFs, Vapour grown carbon fibres.

* Corresponding author: POLYMAT University of the Basque Country UPV/EHU, Avenida Tolosa 72, 20018 Donostia-San Sebastián, Spain.
E-mail address: david.mecerreyes@ehu.es (D. Mecerreyes).

https://doi.org/10.1016/j.progpolymsci.2021.101449

trode active material in energy storage devices is not a recent concept, with early reports dating back to 1970s, where either small molecules (e.g. dichloroisocyanuric acid, quinones) [5,6] or conducting polymers (e.g. poly(aniline), poly(pyrrole)) [7,8] were used as active electrode material in lithium metal-organic batteries. The latter technologies were even developed into two unsuccessful commercial attempts (i.e. Bridgestone-Seiko and Varta batterie/BASF). However, lithium metal-organic batteries were rapidly disregarded due to their lower energy density, shorter cycle life, and higher self-discharge values, when compared to the lithium-ion battery technology, which was commercialized in 1991 by Sony [9,10].

Over the last few decades, tremendous efforts have been directed towards the development of improved redox polymers for lithium ion battery applications [4,11]. Most of literature on redox polymers for energy storage application focuses on organic/inorganic hybrid battery systems such as, alkali metal- or Alkali ion-organic batteries, where redox polymers were generally employed as cathode material in combination with inorganic materials or alkali metals as anodes [4,11,12]. However, this organic/inorganic hybrid battery technology is still employing inorganic intercalation electrodes or lithium/sodium metal as anode, and thus does not take full advantage of the merits of redox polymer electrodes.

In the last years, new batteries technologies just based on organic materials have been gaining more interest within the battery research community, due to the inherent features of redox polymers such as low solubility, processability, flexibility, high rate performance, recyclability, biodegradability, the ability to be 2D or 3D printed and the perspective to prepare them from renewable resources. As for any contemporary technology, whether in development or commercialized, the sustainability and environmental friendliness are important criteria, as highlighted by the introduction of the 17 sustainable development goals by the United Nations, in 2015, in the 2030 Agenda for Sustainable Development. In this regard, redox-active polymers can offer a promising alternative to develop sustainable and efficient energy storage solutions, due to the prospect of recyclability and/or biodegradability of materials. Additionally, their precursor materials are not considered 'scare materials' and could be potentially derived from biomass, and thus offer a path towards low-cost and environmentally benign energy storage solutions. Furthermore, the recent emergence of the 'Internet of Things', smart packaging and clothing as well as mobile devices, has urged the need for low-cost, lightweight, printable and flexible energy storage systems, thus making the development of all-polymer batteries, a highly relevant topic.

The goal of this review article is to provide a comprehensive overview on the state of the art of batteries that are just based on redox polymers, without the use of an inorganic electroactive material. (See Fig. 1) The focus of this review is on recent advances in the development of redox polymers for all-organic battery applications; this differentiates the present review from previous reports in the literature that considered a more diverse material compositions, such as small molecules, inorganics etc [1,3,11–15]. The structure of this review is as follows: First, a succinct update of the development of redox polymers will be given, summarizing the main classes of redox polymers and the recent trends. Second, three types of organic battery configurations are described: all-polymer batteries, polymer-air batteries and polymer redox-flow batteries. In each sections, an exhaustive discussion of the various battery prototypes reported in the literature will be provided. Finally, future perspectives on all-polymer batteries will be given, summarizing the major challenges that still needs to be overcome in order to fully unlock their commercial implementation.

2. Redox polymers

Redox polymers are macromolecules, which are able to be oxidized (lose electrons) and reduced (gain electrons) in a reversible way. They contain electroactive sites or groups that undergo these redox processes, which can be located in the main polymer backbone (e.g. conducting polymers) or as a side-chain (e.g. a polymer bearing a quinone pendant group). Redox polymers are promising candidates to substitute inorganic active materials in battery electrodes due to their low specific weight, low solubility, mechanical and thermal stability and safety. Assessment criteria for electrode materials have been, up to now, mainly focused on their electrochemical performances, especially in terms of specific discharge capacity, energy density that can be reached when incorporated in an energy storage device, and their cycling stability. Redox polymers that are applied as electrode materials in batteries are characterized by their redox potential, capacity, cycle life and rate capability. The specific energy (W h kg^{-1}) of a battery is calculated by the multiplication of the cell voltage (V) and the specific capacity (A h Kg^{-1}). Thus, the higher the cell voltage (potential difference between cathode and anode) and the specific capacity of the active materials, higher will be the energy stored in the battery. The most used redox polymer families in batteries are represented in Fig. 2, depending on their redox potential and specific capacity.

First attempts to incorporate redox polymers as electrodes in batteries started with conjugated redox polymers such as polyacetylene, polypyrrole and polyaniline [16]. However, the electrodes made from these polymers presented relatively low specific capacities (50–150 mAh g^{-1}) and poor cyclability that eventually hindered their research and development. Nowadays, conjugated polymers with higher stability and specific capacity have been developed by increasing the doping level or by introducing redox-active side-chains. The most successful conducting polymer is poly(3,4-ethylenedioxythiophene) (PEDOT) due to its high electronic conductivity and ambient stability [17]. Although it has been used as electrode material in batteries, it is preferred in supercapacitors and hybrid systems as it has high electronic conductivity over a wide potential range (2.5 V to 4.5 V vs. Li/Li^+) and sloping voltage behavior [18].

The initial works with conducting polymers were followed by the application of radical-based redox polymers as electrode materials in batteries. Nishide and coworkers pioneered this field by the application of a polymer containing a nitroxide radical pendant group [19]. Apart from the most used radical moiety, which is based on a nitroxide radical (i.e. 2,2,6,6-tetramethylpiperidine-1-oxyl radical, TEMPO), other radical groups such as galvanoxyl, phenoxyl or hydrazyls have also been incorporated in polymers for battery applications [19–23]. The main advantage of radical polymers resides in their fast electron transfer kinetics, resulting in high rate capability and good cycling stability. However radical polymers generally exhibit low specific capacity (i.e. 50–100 $mAh.g^{-1}$), when compared to other redox polymer family, such as the carbonyl ones.

Carbonyl polymers are an important redox polymer family as it includes a large variety of moieties such as conjugated carboxylates, ketones, quinones anhydrides and imides that covers a wide range of redox potentials (0.8–3.0 V vs. Li/Li^+) and specific capacities (100–280 mAh g^{-1}) [4]. For example, benzoquinone-containing polymers are one of the most attractive ones, due to their high theoretical capacity (496 mAh g^{-1}) and high redox potential of about 2.8–3.0 V vs. Li/Li^+ [24]. Moreover, quinone functionalities can be readily accessible by the (electro)chemical oxidation of bio-inspired polymers such as poly(dopamine), poly(catechol)s, lignins or tannins, etc. . Particularly, lignin and tannin bio-polymers are abundant in nature, making them interesting electrode material candidates, in terms of sustainability. Polyimides are another pop-

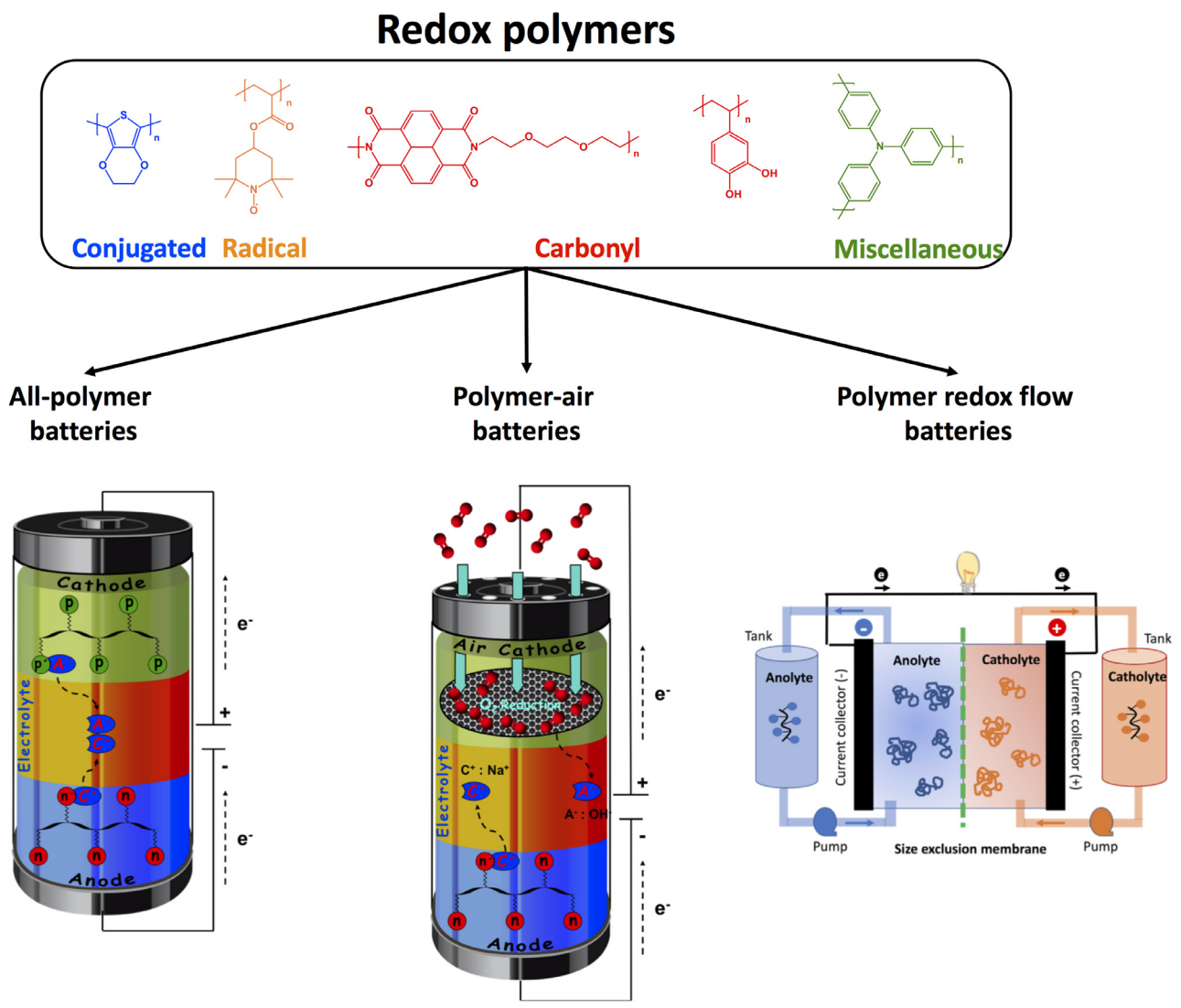

Fig. 1. Review outline, highlighting the different type of redox polymer-based batteries discussed.

ular class of carbonyl-based synthetic polymers used in batteries. Thanks to their well-known redox stability, structural diversity and molecular tunability, their implementation as organic electrode materials in lithium and sodium batteries, as well as redox-active binders in lithium-sulfur batteries has substantially progressed in recent years [25–27].

Apart from the previous three main redox polymer families, other kinds of organic redox moieties have been incorporated into polymers. Some of these redox active groups include phenothiazine, thianthrene and their derivatives, triphenylamine, viologen and organosulfur compounds [15,28–31]. For example, triphenylamine presents a redox potential of 3.8 V vs. Li/Li^+, while viologen undergoes two-successive one-electron redox processes at 1.5 and 2.1 V vs. Li/Li^+.

Therefore, depending on the target application and considering the redox potential, the most appropriate redox polymer can be selected. In the case of an all-polymer battery, a polymer with high redox potential will be chosen for the cathode and another redox polymer with low redox potential as anode, in order to achieve the highest cell voltage, and thus the highest energy density. However, the performance of an all-polymer battery is not only dictated by the potential difference with the two redox polymer electrodes, but other parameters, such as the capacity, the nature of charge carrier and the type of molecular electrolyte solvent, have strong effects on the compatibility, chemical and electrochemical stability of the materials and have to be carefully optimized. The different cell configurations and the importance of the charge carriers are explained in detail in the next section. For polymer redox-flow batteries (pRFB), the principle of cell voltage is the same, but differently from static batteries where the redox-polymer is a solid attached to the current collector, in pRFB, redox polymers are dissolved or suspended in the electrolyte and stored in external tank reservoirs (catholyte and anolyte). Therefore, besides the specific capacity of the polymers, their concentration in the electrolyte will be of paramount importance to get high energy densities and should be considered in this application, as it will be explained in Section 5.

Redox polymers are also promising materials to replace the reactive alkali-metal anodes in metal-air batteries which show safety and cycling stability issues. Thus, a polymer-air battery will consist of an oxygen cathode and a redox polymer anode. As the standard potential of oxygen in acidic water is 1.23 V vs. SHE (it varies with the electrolyte and pH), redox polymers with low potential and good compatibility with oxygen species and protic media are targeted. Due to the recent development of this technology, nowadays there are only a few examples of polymer-air batteries, which

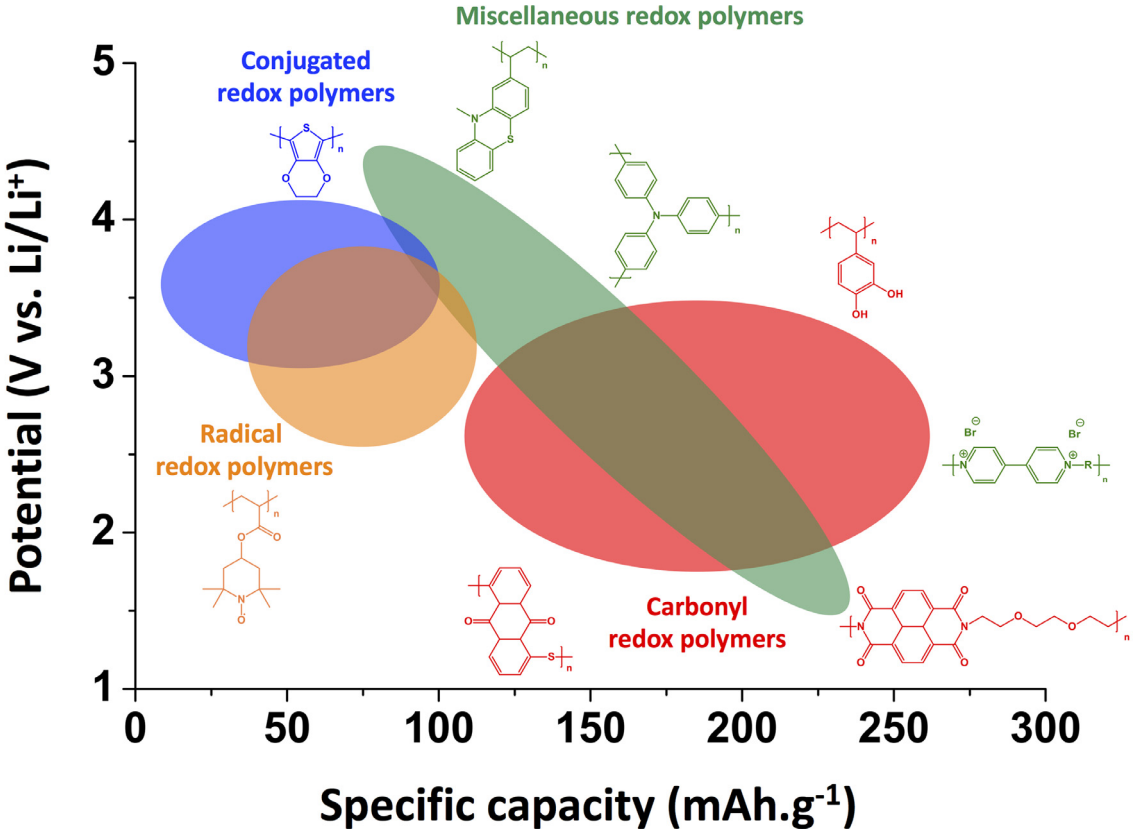

Fig. 2. Relationship between redox potential and specific capacity for the four family of redox polymers : conjugated, carbonyls, radicals and miscellaneous redox polymers.

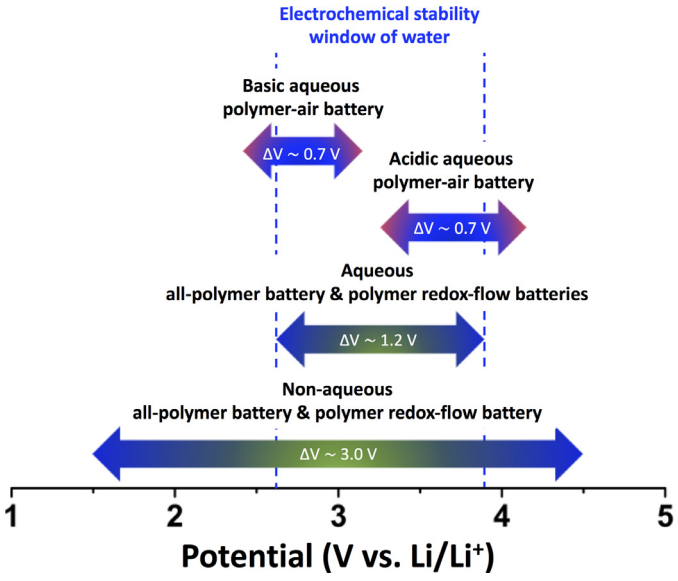

Fig. 3. Theoretical cell voltage accessible for the different redox polymer-based battery systems, reported to date.

are all based in aqueous electrolytes, as it will be described in Section 4.

Fig. 3 shows a summary of the cell voltage accessible, based the redox potential of the variety of redox polymers reported to date and the nature of the electrolyte for the different redox polymer-based battery system previously described. It is worth to mention besides the incorporation of new redox moieties into linear polymers, other macromolecular engineering strategies are being adopted, such as the synthesis of polymer particles [32], covalent organic frameworks [12,33] or conjugated microporous polymers [34], in order to improve the actual performance of redox polymers in batteries.

The redox reactions in redox polymers are associated with a change in the state of charge of the electroactive moiety, enabling fast electron-transfer kinetics. In contrast with redox reactions involved in inorganic redox materials that are related with a change of valence of the transition metal (i.e. cathode material), resulting in slower kinetics [3]. Redox polymers can be classified into three different sub-classes, depending on the type of redox reaction they undergo. Indeed, redox polymers can be either oxidized (lose electrons, resulting in the formation of a positive charge), reduced (gain electrons, resulting in the formation of a negative charge) or both, and are classified as p-type, n-type and b-type, respectively. Fig. 4 illustrates the redox processes associated with n-type, p-type and b-type redox polymers, with the simultaneous shuttling of electro-neutralizing cations, anions, from the electrolyte, respectively.

As an example of a p-type redox polymer, poly(2-vinylphenothiazine) typically undergoes two one-electron oxidation reaction steps, going from the neutral heteroaromatic state to radical cation and then to the formation of the dication, as illustrated in Fig. 4a. During the formation of either the radical cation or the dication species, anion(s) from the electrolyte are transferred to counter-balance the positive charge formed on the redox polymer. It is worth to mention that the second oxidation step to the dication species is not reversible for thianthrene-, phenothiazine-based redox polymers, and has only been reported reversible for dihydrophenazine-based redox polymers [15]. Similarly, other p-type redox polymers, which contains conjugated amine, etheroxide and thioether moities, can also undergoes

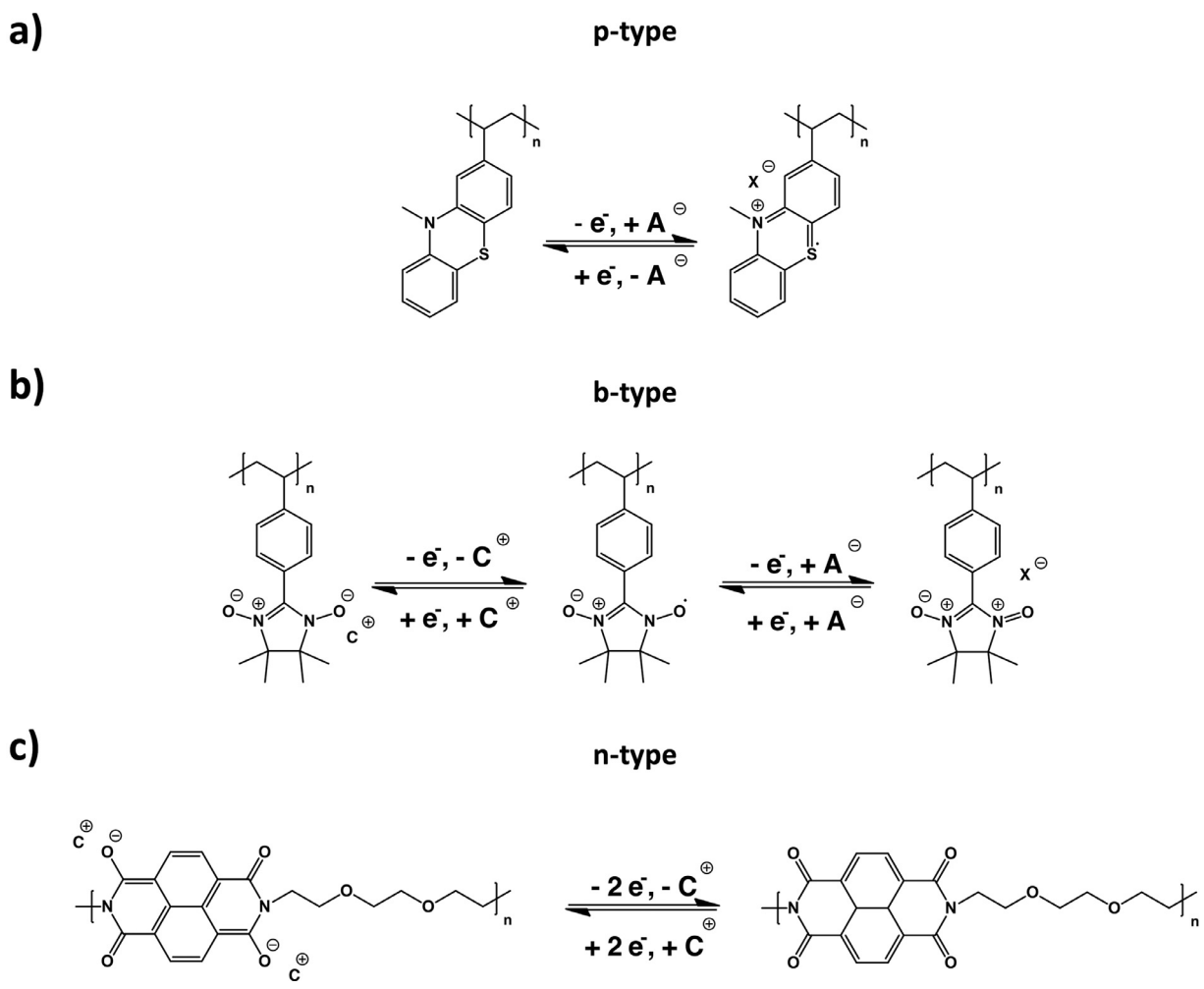

Fig. 4. Redox processes involved in redox polymers, with respect to p-type (a), b-type (b) and n-type (c). C^+ and X^- represent positive and negative charges, respectively, either from the electrolyte or within the redox polymer architecture.

one-electron oxidation reaction to form the corresponding radical cation [1].

On the other hand, poly(1,4,5,8-naphthalenetetracarboxylic bisimide) is a well-known n-type redox polymer, which undergoes two-electron reduction reaction in either one or two steps depending on the electrolyte used. In this case, the naphthlenetetracarboxylic moiety gains two electrons and is reduced to the dianion species, through the enolization of two out of the four available carbonyl groups, as illustrated in Fig. 4c. In this case, the negative charges formed during the enolization process are compensated by shuttling cations from the electrolyte. Other carbonyl-based n-type redox moieties, which undergo similar two-electron redox step, are quinones, anthraquinones, dihydroxy benzenes (catechol), conjugated carboxylate, quinones anhydrides and imides [4].

Finally, b-type redox polymers, where fewer examples are reported, are able to undergo both oxidation and reduction redox reactions, as previously mentioned. As an example, Nishide and co-workers reported a radical polymer with bipolar redox activity, based on Poly[4-(nitronylnitroxyl)styrene] [35]. As illustrated in Fig. 4b, the nitronylnitroxyl moiety can undergoes two one-electron redox reactions, associated with either n-type and p-type doping. In the p-type doping process, the nitroxide radical moiety loses an electron and forms the corresponding oxoammonium cation, which is compensated by an anion from the electrolyte. During the n-type doping process, the nitroxide radical moiety gains an electron and forms the corresponding aminoxyl anion with cation from the electrolyte as counter-charge.

Generally, p-type redox polymer exhibits higher redox potential than the n-type. N-, p-, and b-type redox polymer can be utilized as anode or cathode materials in electrochemical energy storage devices, provided that a satisfactory redox potential difference between them is observed. Additionally, b-type redox polymer can be also employed in a symmetric battery, utilizing the same bipolar polymer in both electrodes.

3. All-polymer batteries

3.1. Introduction

In all-polymer batteries, both anode and cathode electrodes are made of redox polymers of either n-type, b-type or p-type, where the resulting voltage output is based on the potential difference between both redox polymers, as illustrated in Fig. 5. In a special case, symmetric all-polymer battery can also be designed using a b-type redox polymer as both anode and cathode, where the voltage output is generated, this time, by the potential difference between the two redox processes of the b-type redox polymer. To date, voltage outputs, ranging from 0.15 to 2.6 V, were reported for all-polymer batteries, which is still lower than the current lithium-ion battery technology (i.e. 4.5 V), highlighting the actual need for the development of new redox polymers with ultralow or ultra-

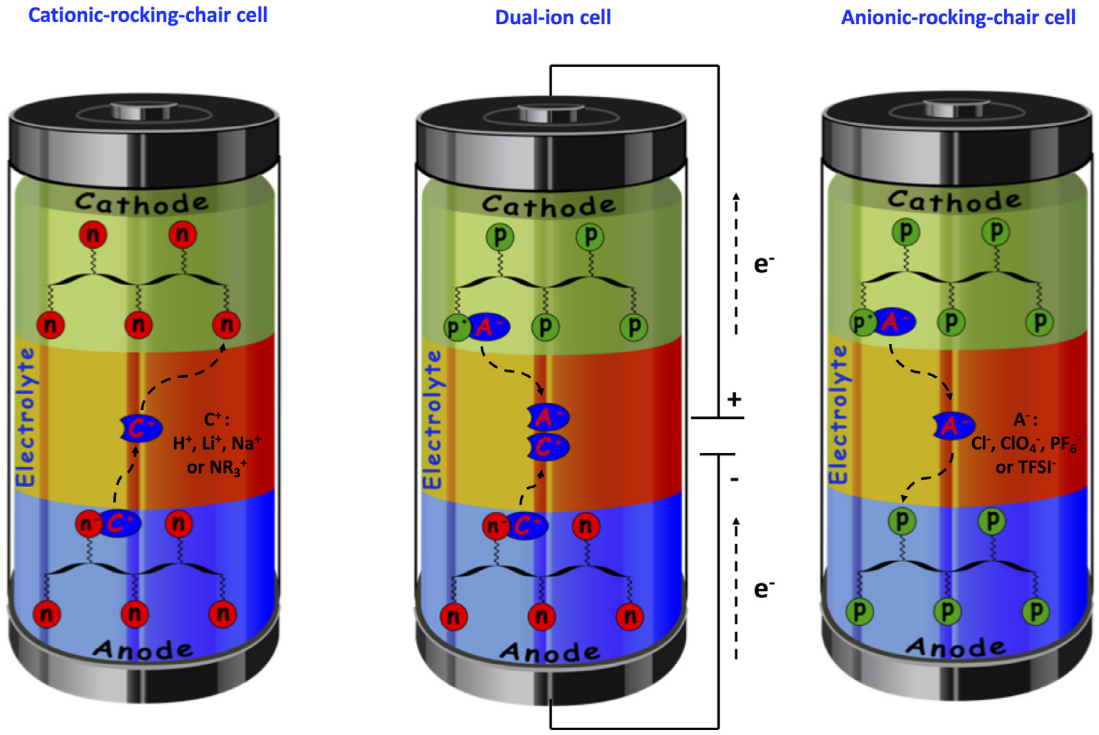

Fig. 5. Cell configuration accessible in all-polymer batteries, via a combination of n-type and/or p-type redox polymers: Cationic rocking-chair cell (left), Dual-ion cell (middle) and Anionic rocking-chair cell.

high redox potentials. Depending on the type of redox polymer (i.e. *n*- or p-type) used as anode and cathode, three main cell configurations are possible in all-polymer battery. The first configuration is based on a cationic rocking-chair concept, where n-type redox polymers are employed as both anode and cathode and cationic charge carriers are used to counterbalance the negative charge formed on the redox polymers. The second configuration is based on the opposite principle, where p-type redox polymers are employed as both anode and cathode and anionic charge carriers are used to counterbalance the positive charge formed on the redox polymer. The last configuration, also known as dual-ion cell concept, is a combination of thereof, where a n-type and a p-type redox polymers are generally employed as anode and cathode, respectively, and both cationic and anionic charge carriers from the electrolyte are used to counter balance the negative and positive charge formed on the n-type and p-type redox polymers, respectively. This last cell configuration generally exhibits higher voltage output, as n-type and p-type possess lower and higher redox potential respectively. However, the ion concentration and thus, the electrolyte properties (ionic conductivity, viscosity, etc.) in dual-ion batteries change during the operation of the battery, demanding higher amount of supporting salt to remain in the optimum concentration range of the electrolyte, in terms of conductivity and transport number. Where in contrast, the ion concentration in rocking-chair cell configuration (n/n and p/p combination) remains fairly constant, thus electrolyte primarily serves as supporting media. Fig. 5 illustrates the different cell configurations accessible with all-polymer batteries.

In the next sections, we will analyse the different all-polymer batteries that have been reported up to date, taking into account the type of redox polymer involved and electrolyte.

3.2. Conjugated redox polymers in all polymer batteries

The development of all-polymer batteries started in the late 1960s [36,37], with the emergence of a new class of materials, known today as conducting polymers [38–43]. Fig. 6 illustrates selected examples of all-polymer battery, using conjugated redox polymers as electroactive materials.

In 1968, Surville et al. was one of the first to introduce the concept of an all-polymer battery, based poly(aniline) (PANI) films with different oxidation states, as both anode and cathode [48]. This cationic rocking-chair battery, which employed a sulfuric acid-based electrolyte, resided on the (de-)doping of poly(aniline) by proton ions to balance the charge formed on the conducting polymer during battery operation. While no cycling data was reported, the all-polymer battery was able to deliver a specific discharge capacity of 13 $mAh.g^{-1}$. A decade later, MacInnes et al. reported an all-polymer battery, based on a dual-ion cell concept, where Li^+ and ClO_4^- ions were used as counter-ions to ensure electrical neutrality of poly(acetylene) films during the n-type and p-type doping processes, respectively [36]. Although, no electrochemical performance of this battery prototype was presented, an initial open circuit voltage of 2.9 V was reported in its charged state [36]. In the same study, MacInnes et al. extended their initial observations on the reversible n-type doping of poly(acetylene) by alkali metal species to non-metallic species, such as tetra-alkylammonium cations, introducing for the first time the concept of all-polymer battery based on a metal-free electrolyte [36]. Again, no battery performance was presented, however, the proposed battery prototype, which was also based on a dual-ion cell concept, exhibited an initial open circuit voltage of 2.5 V, when using n-doped and p-doped poly(acetylene) films as anode and cathode, respectively. Parallelly, Chiang described for the first time an all-polymer battery using a solid-state electrolyte, based on poly(ethylene oxide) containing sodium iodide salt[37]. This solid-state all-polymer battery employed undoped poly(acetylene) as anode and cathode, which relied on (de-)doping of sodium ions and iodide anions, respectively. The battery was operated at 85 °C, due to the ionic conductivity limitations of poly(ethylene oxide)/NaI electrolyte, but was able to de-

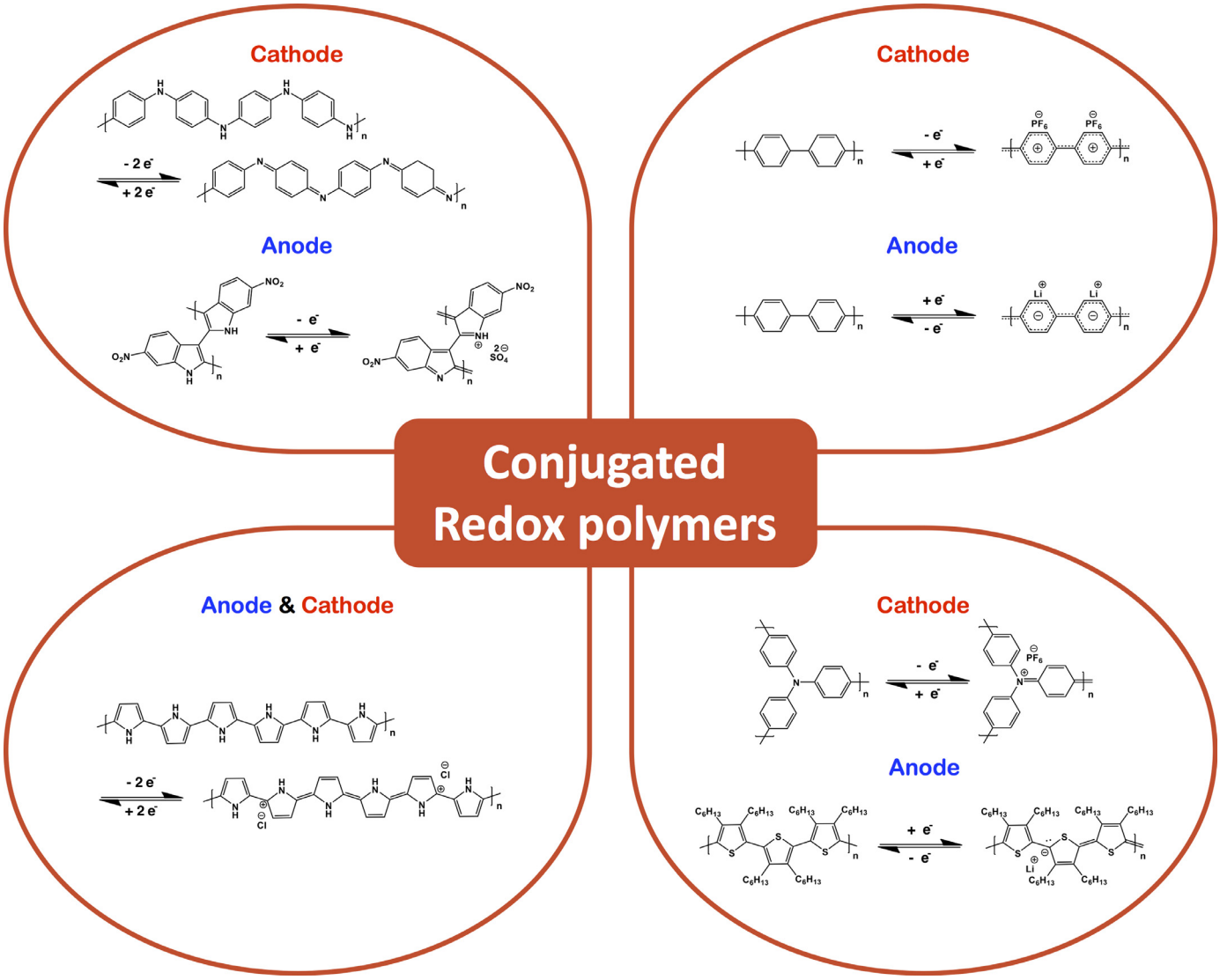

Fig. 6. Examples of all-polymer batteries using on conjugated redox polymers: Top-left ([44]), Top-right ([45]), Bottom-left: ([46]) and Bottom-right ([47]).

liver a specific energy density of 20 $Wh.kg^{-1}$ based on an open circuit voltage ranging from 2.8 to 3.5 V. Shortly after, a similar dual-ion battery was reported using poly(thiophene)films as both anode and cathode materials, delivering a specific discharge capacity of 24 $mAh.g^{-1}$, which corresponds to an energy density of 75 $Wh.kg^{-1}$ based on a discharge voltage of 3.1 V [49]. In 1996, Killian et al. employed the small redox potential difference exhibited between poly(pyrrole) and poly(pyrrole):poly(styrene sulfonate) (i.e. ~ 350 mV) to construct an all-polymer battery using a gel electrolyte based on $LiClO_4$ in poly(acrylonitrile)/ethylene carbonate/propylene carbonate [50]. The proposed all-polymer battery displayed good coulombic efficiencies in the range of 90–95% and no obvious capacity fading over 100 cycles [50]. However, a low specific charge capacity of only 22 $mAh.g^{-1}$ was reached. Following the same redox polymers design strategy, Wallace and co-workers described a textile based all-polymer battery, employing a poly(3′-styryl-4,4′′-didecyloxyterthiophene) (poly(OC_{10}DASTT)) and p-doped poly(pyrrole) (pPy-PF_6), respectively [51]. This anionic rocking-chair battery displayed no capacity decay over 50 cycles, delivering a specific discharge capacity of 35.5 $mAh.g^{-1}$ at a current density of 0.05 $mA.cm^{-2}$. Six years later, Wallace and co-workers proposed another flexible all-polymer battery, using this time poly(pyrrole):para-toluene sulfonic acid (pPy-pTS) and poly(pyrrole): indigo carmine (pPy-IC) as the cathode and anode, respectively [52]. Flexible self-standing electrodes were produced by electropolymerization of the monomeric precursors onto stainless steel plate, which were then peeled-off. This flexible all-polymer battery was able to deliver an initial specific discharge capacity of 39 $mAh.g^{-1}$ at a current density of 0.05 $mA.cm^{-2}$, of which 92% remained after 50 cycles. The dual-ion cell also displayed relatively good rate capability, operating at current densities up to 0.07 $mA.cm^{-2}$. Almost forty years later after Surville et al. [48], proposed the first all-polymer proton battery , Cai et al. reported a dual-ion all-polymer battery, based on poly(5-nitroindole) and poly(aniline) as anode and cathode, respectively [44]. The redox reaction occurring at the anode side resided in the (de-)doping of poly(5-nitroindole) by sulphate ions, while in the cathode side, poly(aniline) was doped with proton ions. The resulting cell exhibited an output voltage of around 1.1 V and was able to deliver a specific discharge capacity of 79 $mAh.g^{-1}$, which corresponds to 94% of the theoretical capacity of the poly(5-nitroindole). Good rate capability was also demonstrated with 82% capacity retention, when increasing current density from 1 to 100 $mA.cm^{-2}$. The all-polymer proton battery displayed a remarkable long-term cycling stability, with only 20% capacity fading upon 32,000 cycles at a current density of 1 $mA.cm^{-2}$ [53].

In 2013, Zhu et al. described the bipolar redox behaviour of poly(para-phenylene) (PPP) and its uses as both cathode and anode materials in an all-polymer battery, using a $LiPF_6$-based electrolyte [45]. Both n-type and p-type doping processes were first assessed separately in lithium metal half-cells. Despite a low coulombic efficiency observed during the initial conditioning cycles, a stable specific discharge capacity of 600 $mAh.g^{-1}$ was then reached for the n-type doping process at a current density of 40 $mA.g^{-1}$, with high coulombic efficiency superior to 98%. Even at an elevated discharging rate of 1280 $mA.g^{-1}$, the PPP anode was able to deliver a specific discharge capacity of 200 $mAh.g^{-1}$, highlighting the high rate capability of the n-type doping process and the potential of the PPP polymer as anode material. Unfortunately, the p-type doping of PPP delivered a lower specific discharge capacity of 80 $mAh.g^{-1}$, when compared to the n-type doping process, likely due to steric hindrance, limiting by the doping degree of polymer chains by bulky anions (i.e. PF_6^-). Surprisingly, the symmetrical PPP organic cell, made anode-limited by design, only exhibited a specific discharge capacity of 153 $mAh.g^{-1}$.

Parallelly to development of new conducting polymers for energy storage applications, attention has also been addressed on the design of advanced redox polymer electrodes in order to enhance their electrochemical performance, and thus the resulting battery. In 2009, Nyström et al. reported the chemical oxidative polymerization of pyrrole on a highly porous cellulose-based substrate, resulting in high surface area cellulose/poly(pyrrole) composite electrode (80 $m^2.g^{-1}$) with tens of nanometre thick poly(pyrrole) layer [46]. An all-polymer battery with an open circuit voltage of 1 V was fabricated using cellulose/poly(pyrrole) composite electrodes with different oxidation states as anode and cathode. This anionic rocking-chair battery displayed a relatively sloping discharge voltage profile [46], inherent characteristics of redox polymer electrodes based on conducting polymers [11]. Nevertheless, this all-polymer battery exhibited high rate capability with 70% retention of the initial discharge capacity, even at a current density up to 600 $mA.cm^{-2}$. Such superior rate performance was attributed by the authors to the high surface area cellulose/poly(pyrrole) composite electrode, as well as the nanometre thickness of the poly(pyrrole) layer.

In 2013, Zhu et al. designed an anode electrode composite via in situ polymerization of 3,4-dihexylthiophene (DHT) with 30 wt.% of vapour grown carbon fibres (VGCFs) [47]. The electrochemical performance of the resulting PDHT/VGCFs anode electrode was assessed first in a lithium metal half-cell, delivering a stable specific discharge capacity around 290 $mAh.g^{-1}$ (240 $mAh.g^{-1}$,after subtracting capacity contribution from VGCFs) after some initial conditioning cycles. This electrode also exhibited good rate capability, reaching specific discharge capacities of 215 $mAh.g^{-1}$ and 120 $mAh.g^{-1}$ at a current density of 200 $mA.g^{-1}$ and 400 $mA.g^{-1}$, respectively. An all-polymer battery was constructed using PDHT and poly(triphenylamine) (PTPAn), as anode and cathode electrodes, respectively, attaining a charging voltage plateau of $\sim$ 3 V. Despite, no long-term cycling performance was reported, the resulting dual-ion PDHT/VGCFs|| PTPAn cell delivered a reversible specific discharge capacity of $\sim$ 250 $mAh.g^{-1}$ at a current density of 40 $mA.g^{-1}$.

The implementation of conducting polymers as electrode materials for battery application has been hampered because of their inherent drawbacks, such as low capacity and limited cycle life. Additionally, all-polymer battery based on conducting polymers tends to exhibit a rather sloping voltage profile, as highlighted in Fig. 7, since as the redox potential of conducting polymers is highly dependent of its doping level, due to conjugated system between each redox active moiety, which varies during battery cycling. Consequently, research on electrode materials based on non-conjugated redox polymers has been increasingly attracting interest, and is the focus of the following discussions in the proceeding sections.

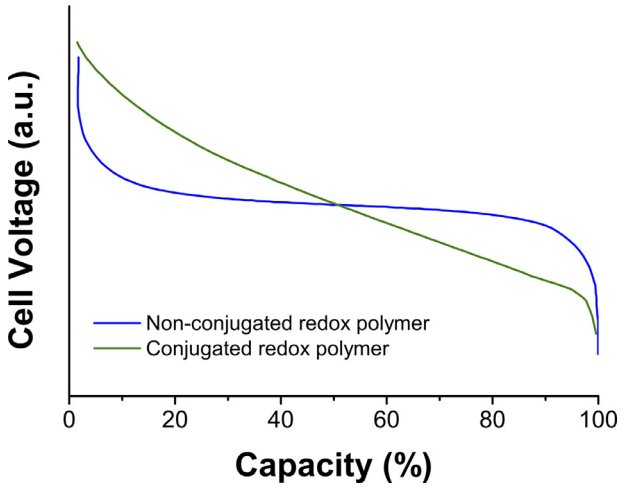

Fig. 7. Typical discharge voltage profiles of all-polymer batteries based either on conjugated redox polymers or non-conjugated redox polymers.

Table 1 summarizes all all-polymer battery prototypes reported to date using conjugated redox polymers.

3.3. Carbonyl redox polymers in all polymer batteries

Carbonyl redox polymers have been intensively studied over the last two decades as organic electrode materials for energy storage application. The vast majority of the literature reported to date on carbonyl redox polymers focused on their application as cathode material in hybrid battery systems, such as alkali metal/ion-organic batteries (Lithium and Post-Lithium battery technologies) [1,4,11]. The few examples of carbonyl redox polymers in all-polymer battery, which are based on the well-known quinone and imide redox functionalities, will be discussed in this section and are illustrated in Fig. 8.

3.3.1. Quinone-based redox polymers

In 2013, Deng et al. reported a sodium-ion battery based on the well-known poly(anthraquinonyl sulphide) (PAQS) and a poly(triphenylamine) (PTPAn), as anode and cathode, respectively [59]. It is noteworthy that this Na-ion battery is actually based on a dual-ion cell concept, since PTPAn is a p-type redox polymer and therefore resides on the (de-)doping of anions from the electrolyte to ensure electrical neutrality. The all-polymer battery, based on PTPAn and PAQS polymers, exhibited an average output voltage of 1.8 V, delivering a specific discharge capacity of 220 $mAh.g^{-1}$ at a current-rate (C-rate) of 1C, indicating 98% utilisation of the anode capacity. The dual-ion battery displayed also high rate capability and excellent long-term cyclability, with 85% retention of its initial discharge capacity upon 500 cycles at a C-rate of 8C, corresponding to a (dis-)charging time of 7.5 min.

Inspired by the work of Surville et al. [48], Sjödin and co-workers proposed, in 2016, an all-polymer proton battery using conducting redox polymers (CPRs) based on quinone functionality [64]. This new design approach consists in covalently attaching a redox active pendant groups to a conducting polymer backbone. It is noteworthy that the matching between the redox potential of the redox active pendant groups and either the *n*- or p-doped potential range of the conducting polymer is of a crucial importance for the redox processes, as any potential mismatch results in limited utilization of redox active pendants. The present strategy allows the design of carbon additive-free polymer electrodes that are soft, light-weight and flexible in nature, which also brings

Table 1
Overview of all-polymer batteries based on conjugated redox polymers.

Cell type	Anode Theoretical capacity ($mAh.g^{-1}$) [a]	Cathode Theoretical capacity ($mAh.g^{-1}$) [a]	Electrolyte	Output voltage (V)	Active material loading ($mg.cm^{-2}$)	Specific capacity ($mAh.g^{-1}$)	Capacity retention, cycle numbers, rate or current density	Ref
Cationic	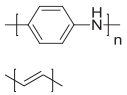	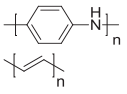	H_2SO_4	–	–	13	-,-,-	[48]
Dual-ion	-	-	0.3 M $LiClO_4$	–	–	–	-,-,-	[36]
Dual-ion	-	-	0.5 M n-Bu_4NClO_4 in PC; 0.3 M n-Bu_4NPF_6 in THF	–	–	–	-,-,-	[36]
Dual-ion	-	-	PEO-NaI	2.8–3.5	–	–	-,-,-	[37]
Dual-ion	-	-	0.2 M $TBABF_4$ in ACN	3.01	0.13 mg	24	-,-,-	[49]
Anionic	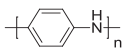 **460 mC**	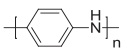 790 mC	0.1 M TEAP in PC	0.4	–	–	60%,-,1 C	[54]
Dual-ion	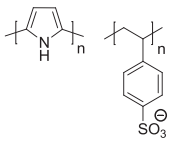 **71**	 138	PAN, $LiClO_4$, EC PC	0.4	–	22	~100%, 100,-	[50]
Anionic	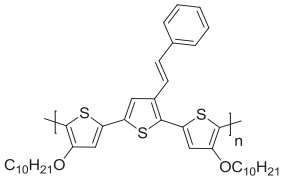 -	 -	1.0 M $LiPF_6$ in 1:1 (v/v) EC:DMC	~0.8	~1 (anode)	39	100%,50,0.05 $mAcm^{-2}$	[51]

(*continued on next page*)

Table 1 (*continued*)

Anionic	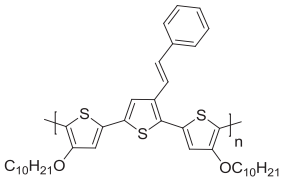 -	 -	1.0 M $LiPF_6$ in 1:1 (v/v) EC:DMC	0.52	–	45.2	59.1%,150,-	[55]
Dual-ion	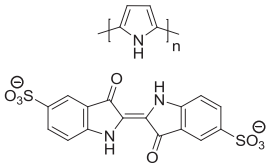 -	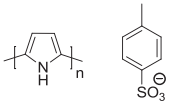 -	1 M $LiPF_6$ in EC:DMC 1:1 (v/v)	1.5	–	36	92%,50,0.05 mA cm^{-2}	[52]
Cationic	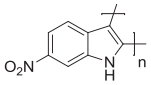 84	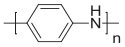 -	H_2SO_4 40%	1.1	–	79	80%,32,000,1 $mAcm^{-2}$	[44]
Dual-ion	 -	 -	1 M $LiPF_6$ in EC:DMC:EMC 1:1:1 (v/v/v)	3	–	153 (anode-limited)	63%,60,40 mA/g	[45]
Anionic	 Reinforced cellulose nanofibers -	 Reinforced cellulose nanofibers -	2.0 M NaCl	1	18.75 mg	33	94%,100, 600 $mAcm^{-2}$	[46]
Dual-ion	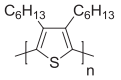 106	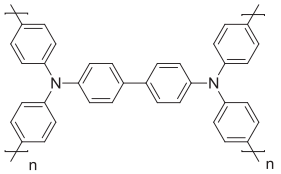 -	1 M $LiPF_6$ in EC:DMC:EMC 1:1:1 (v/v/v)	2.35	–	250 (anode-limited)	-,-,-	[47]

(*continued on next page*)

Table 1 (*continued*)

Cationic	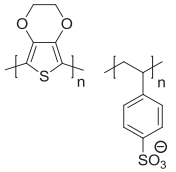	-	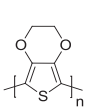	-	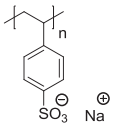	~0.3	–	–	-,-,-	[56]
Cationic	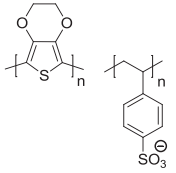	-	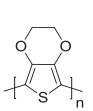	-	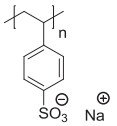	0.82–0.85	–	–	-,-,-	[57]
Dual-ion	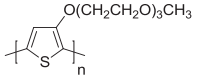	-	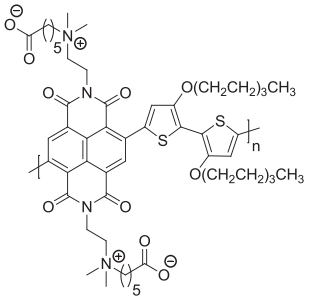	-	-	0.1 NaCl in H_2O	1.4	–	21.3 (p-type) , 25.9 (n-type)	-,-,-	[58]

[a] Theoretical capacity of each electrode, individually. The theoretical capacity of the limiting electrode in the full cell is indicated in bold.

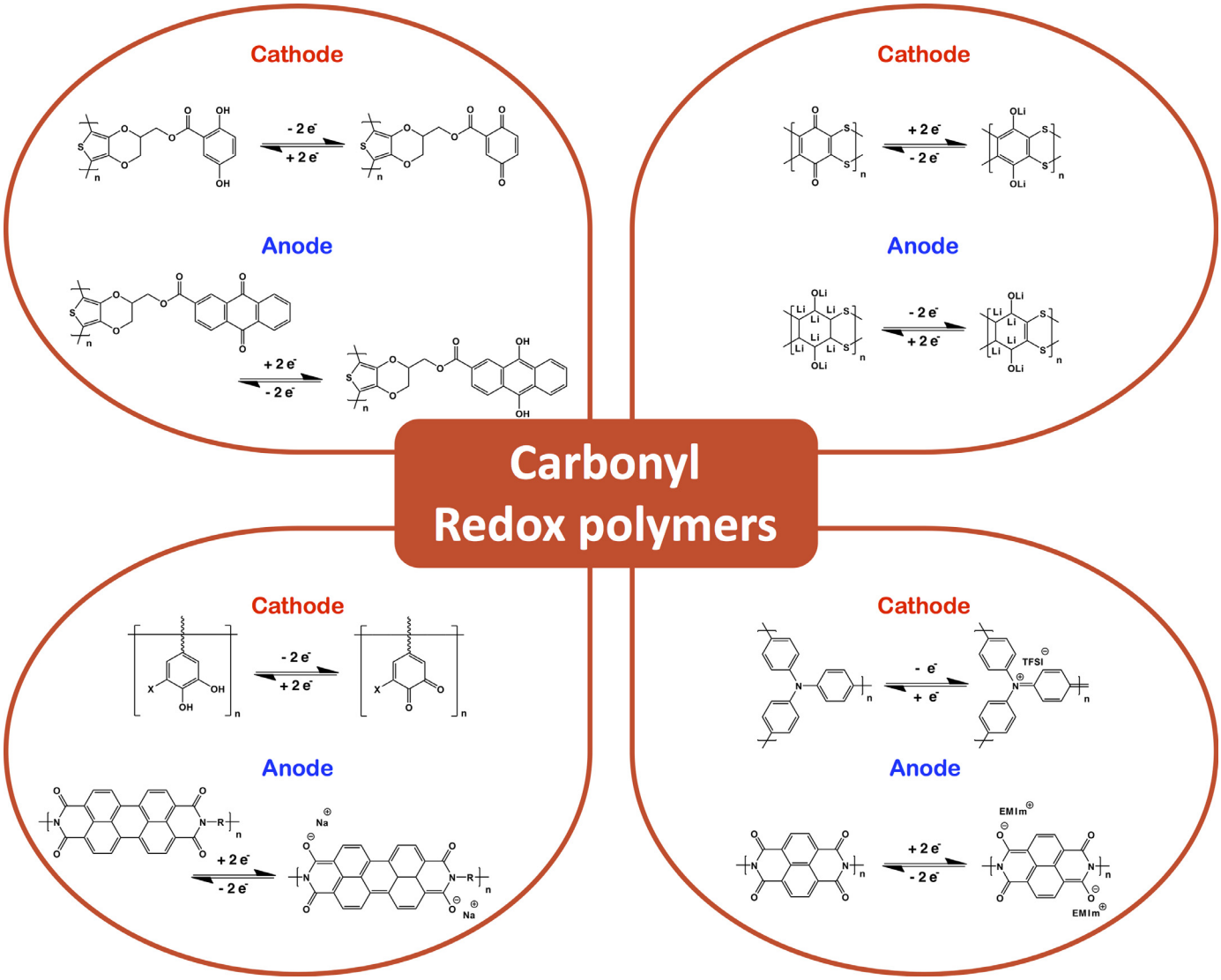

Fig. 8. Examples of all-polymer batteries using on carbonyl redox polymers: Top-left ([60]), Top-right ([61]), Bottom-left: ([62]) and Bottom-right ([63]).

about great opportunities to make wearable, flexible, foldable and printable advanced batteries. In the present study, a hydroquinone and a dimethoxy-substituted benzoquinone pendant groups, tethered to the poly(pyrrole) backbone, were used as cathode and anode, respectively [64]. The first proof-of-concept all-polymer proton battery based on CPRs electrode pairs exhibited only a low output voltage of 0.15 V, due to the inherent small redox potential difference between the two quinone derivatives used. Building on this proof-of-concept, Sjödin and co-workers developed two new CPRs, based this time on anthraquinone (PEDOT-AQ) and benzoquinone (PEDOT-BQ) redox moieties [60]. (See Fig. 8) The resulting all-polymer proton battery displayed a slightly higher average output voltage of 0.5 V. This new CPRs-based all-polymer proton battery was assessed in both anode and cathode limited design, in order to evaluate separately the electrochemical performance of both PEDOT-AQ and PEDOT-BQ electrodes, respectively. Although, the PEDOT-BQ showed high degree of instability and fast capacity fading, in anode-limited design (i.e. PEDOT-AQ), the proton battery was able to deliver 78%, 68% and 19% of its theoretical capacity (i.e. 103 $mAh.g^{-1}$) at a C-rate of C/2, 3C and 160C, respectively, highlighting the relatively good rate capability of this CPRs-based battery. Additionally, a decent cycling stability was also demonstrated with only 2% capacity fading upon 100 cycles at a C-rate of 3C. The authors also mentioned that the PEDOT-AQ anode was able to cycle for 1000 cycles with no obvious instability, if the PEDOT-BQ cathode was repetitively replaced with a fresh electrode. However, only post-cycling cyclic voltammograms of the PEDOT-AQ electrode were shown, with no concrete capacity data reported.

It is well-known that the (de-)doping of hydroquinone based redox polymer is facilitated when protons are used instead of lithium or sodium ions as shuttling ions, resulting in much higher redox potential in the former case [65,66]. However, the restricted potential stability window of aqueous electrolytes (~1.23 and ~2 V for pure water and typical salt-in-water electrolytes, respectively, owing to the hydrogen and oxygen evolution reactions) limits the number of redox functionality accessible, and thus, results in lower energy density battery due to the low potential difference between the organic redox polymer electrode employed. To overcome these limitations, Sjödin and co-workers proposed a new design strategy of redox polymers, based on a so-called "proton-trap technology" in 2017 [67,68]. This technology resides on the synthesis of random copolymer, where a proton acceptor monomer, such as pyridine, is copolymerized with a hydroquinone-based monomer. The proton acceptor functionality of the pyridine allowed to decouple the proton (de-)doping of the hydroquinone units from the electrolyte chemistry, and thus, from the organic redox polymer

counter electrode. Unfortunately, this "proton-trap technology" was only demonstrated so far in hybrid battery systems, such as alkali metal/ion-organic batteries. One year later, Karlsson et al. developed a novel protic electrolyte based on nonstoichiometric protic ionic liquid mixtures for application in all-polymer batteries [69]. They employed this novel protic electrolyte in an all-polymer battery, where CRPs based on 1,4-naphthoquinone and hydroquinone functionalities were used as anode and cathode, respectively. This all-polymer proton battery exhibited a cell potential of 0.45 V. However, the cell showed fast capacity fading, with only 60% of its initial specific capacity over 100 cycles. The authors attributed the capacity fading to degradation and/or dissolution of hydroquinone-based CRPs electrode, as evidenced by a coulombic efficiency over 100%.

Recently Sjödin and co-workers developed a new method to prepare conducting polymer and/or CPRs electrodes, through post-coating polymerization technique by either chemical or electrochemical means. It is noteworthy that this method requires the synthesis of trimeric precursor, as the post-coating polymer was not success with typical monomeric precursors. Two new CPRs electrodes, based on hydroquinone and naphthoquinone functionalities, were developed using this new method for application in aqueous all-polymer batteries. The resulting proton rocking-chair battery displayed an average output voltage of 0.4 V and delivered an initial specific discharge capacity of 60 mAh.g-1, which corresponds to 80% of its theoretical capacity (i.e. anode-limited by design). The all-polymer battery exhibited a moderate cycling stability with only 50% capacity retention after 500 cycles under galvanostatic cycling at a C-rate of 3C.

In 2018, Xie et al. described the synthesis of a poly(2,3-dithiino-1,4-benzoquinone) (PDB) for use as both anode and cathode materials in an all-polymer battery [61]. (See Fig. 8) During discharge, the PDB polymer undergoes an enolization reaction of two carbonyl groups at the cathode side, with the incorporation of two lithium ions to preserve polymer neutrality. For its use as an anode material, the PDB polymer needed to be prelithiated, through the reduction of all unsaturated carbon atoms, which will be subsequently delithiated during the discharge process. It is noteworthy that as highlighted by the migration of lithium ions, back and forth between the two electrodes, this symmetric PDB cell is based on a cationic rocking-chair concept, similar to lithium-ion battery technology. The electrochemical performance of both cathodic and anodic PDB electrodes was first assessed separately in lithium metal half-cells, delivering specific discharge capacities of 255 mAh.g^{-1} and 1076 mAh.g^{-1}, respectively. The difference in capacity between these two redox processes was linked with the number of electrons involved in each redox reactions; two-electron reaction vs. six-electron reaction for the cathodic and anodic redox processes, respectively. Additionally, it was reported that the PDB cathode exhibited high rate capability and long-term stability, still delivering a high specific charge capacity of 161 mAh.g^{-1} and 80% capacity retention after 1000 cycles at an ultra-high applied current density of 1.5 A.g^{-1}. Surprisingly, the symmetric PDB all-polymer battery displayed a moderate cycling stability, retaining only 68% of its initial capacity after 250 cycles at a current density of 0.5 A.g^{-1}. Similar observation was made in terms of the rate capability, pointing out that the limiting factor might be due to the poor electrochemical performance of the PDB anode material. Having a single redox polymer as both cathode and anode electrode presents a significant benefit in terms of battery design, although on the other hand, generating a high voltage output from a b-type redox polymer is very challenging task for chemistry design point of view.

Like in lithium-ion batteries technology, the pursuit for safer energy storage solutions has driven the development of solid-state electrolytes due to their inherent advantages, such as low volatility/flammability, high anodic and thermal stabilities. Following this research direction, Zhu et al. developed a solid-state electrolyte based a succinonitrile plastic crystal containing sodium perchlorate [70]. They employed this novel solid-state electrolyte in an all-polymer battery, consisting of a poly(anthraquinonyl sulphide) anode and a poly(aniline-r-nitroaniline) cathode. This solid-state all-polymer battery exhibited an average output voltage of 1.6 V at room temperature and was able to deliver a specific discharge capacity of 200 mAh.g^{-1} at a current density of 50 mA.g^{-1}, which corresponds to 89% of its theoretical capacity. (i.e. anode-limited by design) Unfortunately, the cell displayed low cycling stability with only 80% capacity retention upon 50 cycles.

3.3.2. Imide-based redox polymers

In 2018, a low-cost aqueous all-polymer battery was proposed by Mecerreyes and co-workers [62], based on a novel perylene polyimide anode and a previously reported poly(3,4-ethylenedioxythiophene)-lignin biopolymer cathode[71,72]. The electrochemical performance of the perylene polyimide was first assessed using a sodium sulphate aqueous electrolyte in a half-cell configuration, exhibiting astonishing rate capability and long-term cyclability, with a discharge capacity of 54 mAh.g^{-1} and a 98% capacity retention over 2000 cycles at a high C-rate of 600C. The superior electrochemical performance of the perylene polyimide, compared to than that of its naphthalene analogue, was likely due to its enhanced electronic and ionic conductivity because of the higher conjugation of the perylene aromatic ring and incorporation of ethylene oxide comonomers, respectively. The resulting all-polymer battery displayed slightly inferior cycling performance, although, still delivering 85% of its initial capacity after 800 cycles at a C-rate of 100C.

In their succeeding work, they developed an all-polymer battery, based on poly(1,4,5,8- naphthalenetetracarboxylic diimide-1,2-diethoxyethane) (termed simply as poly(imide)) and poly(dopamine acrylamide-r-2-acrylamido-2-methylpropane sulfonic acid) (termed simply as poly(catechol)) as anode and cathode, respectively [73]. In addition, various charge carriers such as Li^+, Zn^{2+}, Al^{3+}, and Li^+/H^+, compared to Na^+/H^+ as in the previous example [62], were investigated. Both poly(catechol) and poly(imide) exhibited stable electrochemical behavior in all of the aforementioned aqueous electrolytes, suggesting that they can be applied as the universal organic electrodes in numerous energy storage technologies. Interestingly, an increase in cell voltage was observed, going from 0.58 to 0.74, and further to 0.89 V, when the type of charge carrier changed from Li^+ to Zn^{2+}, and to Al^{3+}, attributed to distinctive strength of metal cation–redox core ionic interactions of electrode partners with different charge carriers based on their n-type redox behavior. Moreover, full cell with mixed Li^+/H^+aqueous electrolyte, exhibited the highest cell voltage of 0.95 V with good cycling stability (75% capacity retention over 1000 cycles at 5 A g^{-1}). The concurrent high specific capacity (85 mAh g^{-1}), high cell voltage (0.95 V), and ultrafast kinetics (working at 500 A g^{-1}, which corresponds to 0.1 s charge or discharge), endowed an impressive energy density of $\sim$ 80.6 Wh kg^{-1}, where the high value of $\sim$10 Wh kg^{-1} was still achieved at the unprecedented power density of $\sim$348 kW kg^{-1} based on the total mass of both electrodes and the consumed salt. This overall performance was far superior than most of the reported all-polymer aqueous stationary batteries and signifies the importance of macromolecular engineering approaches to improve the energy storage performance for the design of next-generation batteries.

Using the well-known poly(1,4,5,8-naphthalenetetracarboxylic bisimide) (PI-5) [74], Zhang et al. proposed an ammonium-based aqueous all-polymer battery [75], by coupling it with the most studied radical redox polymer cathode, poly(2,2,6,6-

tetramethylpiperidine-N-oxyl)methacrylate polymer (PTMA) [76]. The PI-5 polymer has been intensively investigated as cathode material for lithium metal-organic batteries [27,77], but never with a metal-free electrolyte. The redox activity of the PI-5 polymer was investigated using various aqueous electrolytes containing different cations (NH_4^+, Li^+, Na^+) with the same anion (SO_4^{2-}), separately. The $(NH_4)_2SO_{4(aq)}$ electrolyte displayed faster redox kinetics, when compared to its lithium or sodium electrolyte analogues, resulting in higher specific discharge capacity and good rate capability in a half-cell configuration. Such result was attributed to the differences in ionic size of the hydrated cation charge carriers, described in the following order: $Li^+ > Na^+ > NH_4^+$. The resulting dual-ion aqueous battery, composed of PI-5 and PTMA as anode and cathode respectively, exhibited similar performance, with 72% retention of its initial specific discharge capacity of 136 $mAh.g^{-1}$, when increasing current density from 0.5 $A.g^{-1}$ to 10 $A.g^{-1}$. The device was able to deliver maximum energy and power densities as high as 51 $Wh.kg^{-1}$ and 15.8 $kW.kg^{-1}$ (5.1 $Wh.kg^{-1}$), respectively. Additionally, excellent long-term cycling stability of the dual-ion battery was also demonstrated, delivering 86% of its initial specific discharge capacity after 10,000 cycles, even at an elevated current density of 5 $A.g^{-1}$.

Taking advantage of the faster redox kinetics of redox polymers, the development of new electrolyte has attracted a lot of attention for application in all-polymer battery at low and ultralow operating temperatures. In 2018, Dong et al. described an all-polymer battery based on ethyl acetate electrolyte containing lithium bis(trifluoromethanesulfonyl)imide salt, operating at temperature as low as −70 °C [78]. The all-polymer battery was composed of the poly(1,4,5,8-naphthalenetetracarboxylic bisimide) and the poly(triphenylamine) (PTPAn) as anode and cathode, respectively. The device exhibited an average output voltage of 1.2 V and was able to deliver a slightly penalized specific discharge capacity of 69 $mAh.g^{-1}$ (70% capacity retention) at −70 °C at a low C-rate of 0.5 C, compared to that attained one at 25 °C (99 $mAh.g^{-1}$). As a comparison, a lithium-ion cell, based on intercalation materials electrodes, was only able to retain 20% of its specific discharge capacity, when decreasing operating temperature from 25 °C to −70 °C [78]. Using redox polymers as anode and cathode (i.e. PI-5 and PTPAn, respectively), Zhan and co-workers reported an all-polymer battery, which employed a pure ionic liquid as electrolyte, 1-ethyl-3-methylimidazolium bis(trifluoromethylsulfonyl)imide (EMImTFSI) [63]. (See Fig. 8) The all-polymer battery displayed high rate capability with 70% retention of its initial discharge capacity, when increasing C-rate from 1C to 200C, corresponding to 1 h and 12.6 s (dis-)charging time, respectively. Additionally, the cell exhibited excellent cycling stability with only 25% capacity loss upon 5000 cycles at an elevated C-rate of 20 C. Enhanced cycling stability over 200 cycles was demonstrated, when decreasing battery operation temperature from 25 °C to −10 °C. A year later, Zhan and co-workers also developed an ternary electrolyte system, based on an acetonitrile (ACN) and methyl acetate (MA) mixture containing 1 M EMImTFSI [79]. The resulting PI-5|EMImTFSI/MA/ACN|PTPAn cell was able to deliver 79% of its initial capacity when decreasing operating battery temperature from 20 °C to −80 °C. Additionally, this dual-ion cell exhibited outstanding long-term cycling stability under an applied C-rate of 5C, with 86% and 98% capacity retention over 2000 cycles at 20 °C and −60 °C, respectively.

Recently, Zhou et al., described the preparation of highly porous redox polymer composite nanofiber electrode (i.e. PI/NDC/CNT), based on carbon nanotubes (CNTs), nitrogen-doped carbon and poly(1,4,5,8-naphthalenetetracarboxylic bisimide-1,2-para-phenyl), via an electrospinning method [80]. The electrochemical performance of the PI/NDC/CNT electrode was first assessed in a half-cell configuration using an 1.0 M $(NH_4)_2SO_4$ aqueous electrolyte, delivering specific capacities of 161 $mAh.g^{-1}$ at a current density of 0.5 $A.g^{-1}$. The PI/NDC/CNT electrode displayed good rate capability, with 76% capacity retention when increasing current density from 0.5 to 10 $A.g^{-1}$. Additionally, the PI/NDC/CNT electrode exhibited good long-term cycling stability, with 98 % capacity retention after 5000 cycles at 5 $A.g^{-1}$. Moreover, an aqueous all-polymer battery was also constructed by coupling the PI/NDC/CNT anode electrode with a polyaniline/carbon nanofiber composites, yielding to rather slopping output voltage of ∼1.0 V. The aqueous all-polymer battery was able to deliver a high specific energy density of 114 $Wh.kg^{-1}$ at a power density of 18.6 $kW.kg^{-1}$.

Table 2 summarizes all all-polymer battery prototypes reported to date using carbonyl redox polymers.

3.4. Radical-based redox polymers

In 2002, Nakahara et al. proposed a new class of redox polymers based on a stable nitroxyl radical, 2,2,6,6-tetramethylpiperidinyl-N-oxyl (TEMPO), demonstrating first their potential as cathode material in a lithium-polymer battery, delivering a specific discharge capacity of 70 $mAh.g^{-1}$, of which 98% remained after 500 cycles at a current density of 1 $mA.cm^{-2}$ [76]. Fig. 9 highlights some key examples of all-polymer batteries using radical redox polymers.

In 2007, Nishide and co-workers developed, for the first time, n-type radical polymers, based on nitroxylstyrene radicals [82] and shortly after on galvinoxylstyrene radicals [20]. With the latter, an all-polymer battery was constructed using a p-type poly(TEMPO-substituted norbornene) as cathode, yielding to an average output voltage of 0.66 V. This all-polymer radical battery displayed high rate capability, enabling charging at a C-rate of 360C, corresponding to a charging period of 10 s. Additionally, satisfactory cycling stability was observed, with 75% capacity retention after 250 cycles.

Shortly after, a bipolar radical polymer, poly(4-(nitronylnitroxyl)stryrene), was designed by the same research group for application as both anode and cathode materials [35]. The poleless battery was able to deliver an initial specific discharge capacity of 44 $mAh.g^{-1}$ (i.e. based on the weight of redox polymers in both electrodes) that corresponds to 86% of its theoretical capacity with an average output voltage of 1.3 V. Good cycle life was reported with 67% of its initial capacity remained after 250 cycles at a C-rate of 10C. Additionally, an tetrabutylammonium-based rocking-chair type battery was also reported, by coupling the same bipolar poly(4-(nitronylnitroxyl)stryrene) polymer with the previously reported n-type poly(galvinoxylstyrene), yielding this time to an average discharge voltage of 0.6 V [35]. This tetrabutylammonium ion battery exhibited even better cycling stability, retaining 91% of its initial capacity. In the search for safer energy storage solutions, Nishide and co-workers synthesised a novel radical polymer based on poly(2,2,6,6-tetramethylpiperidinyloxyl-4-acrylamide) (PTAm), designed to operate in aqueous electrolytes as compared to in traditional flammable organic electrolytes [83,85]. (See Fig. 9) PTAm displayed outstanding long-term cycling stability in a half-cell configuration, delivering an initial specific discharge capacity of 110 $mAh.g^{-1}$, of which 97% remains after 1000 cycles at a high c-rate of 60C [85]. Such performance was attributed to the good swelling properties of the polymer in the $NaBF_4$/water electrolyte, yet not become dissolved into the aqueous electrolyte. The authors also demonstrated the cycling performance of an aqueous all-polymer battery using the present PTAm polymer in conjunction with a viologen-based redox polymer anode, poly(N-4–4′-bipyridinium-N-decametylene dibromide) (PV10), yielding to an average output voltage of 1.2 V. The anionic rocking-chair battery showed good long-term cycling stability, although slightly inferior than that of the PTAm half-cell, with 80% capacity retention after 2000

Table 2
Overview of all-polymer batteries based on carbonyl redox polymers.

Cell type	Anode Theoretical capacity (mAh.g^{-1}) [a]	Cathode Theoretical capacity (mAh.g^{-1}) [a]	Electrolyte	Output voltage (V)	Active material loading (mg.cm^{-2})	Specific capacity (mAh.g^{-1})	Capacity retention, cycle numbers, rate or current density	Ref
Dual-ion	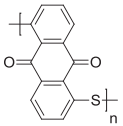 **224** 224	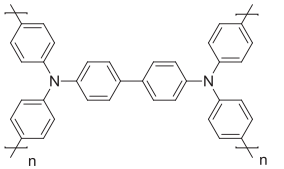 109 109	$NaPF_6$ saturated in DME:DOL 1:1 (v/v)	1.8	–	220	85%, 500, 8C	[59]
Cationic	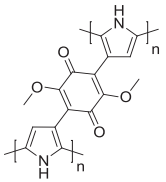 - -	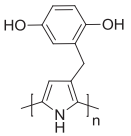 - -	1.0 M $NaNO_3$ (pH 2.20)	0.15	–	–	-,-,-	[64]
Cationic	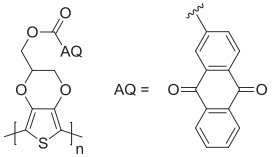 **132** 132	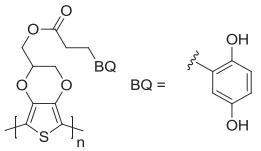 160 160	2-fluoropyridinium triflate/2-fluoropyridine	0.5	0.25–1.5 mg	103	79%,150, 3C	[60]
Cationic	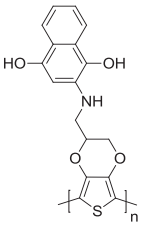 - -	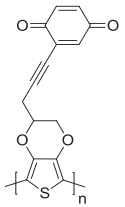 - -	MeTriHTFSI ($x = 30\%$)	0.45	–	100	60%,100,140C	[69]

(*continued on next page*)

Table 2 (*continued*)

Cationic	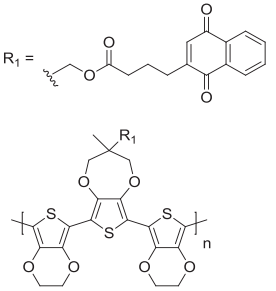 **75**	75	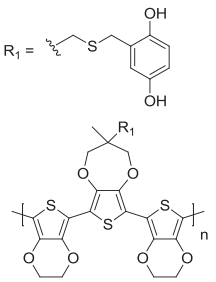 87	87	1 M $H_2SO_{4\ (aq)}$	0.4	2	60	50%, 500, 3C	[81]
Cationic	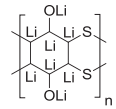 - -		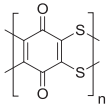 **319** 319		1 M LiTFSI in DOL:DME 1:1 (v/v)	~2.0	0.27–0.63 mg	174	68%,250,0.5 $A.g^{-1}$	[61]
Dual-ion	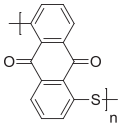 - -		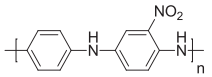 - -		5 mol% $NaClO_4$ in succinonitrile	1.7	~4	200	80%,50,50 $mA.g^{-1}$	[70]
Cationic	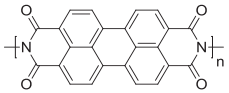 138	138	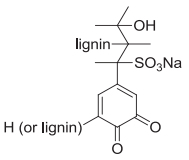 -	-	1 M Na_2SO_4 and 0.1 M $HClO_4$	1.0	0.5 (anode) 1.2 (cathode)	53 (10C), 39 (200C)	85%,800,100C	[62]
Cationic	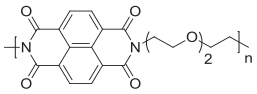 166	166	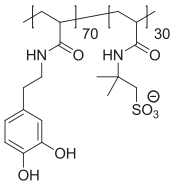 180	180	2.5 M $LiNO_3$, $ZnSO_4$, $Al(NO_3)_3$ or 2.5/0.25 M $LiNO_3/H_2SO_4$	0.58(Li^+) 0.74(Zn^{2+}) 0.89(Al^{3+}) 0.95 (Li^+/H^+)	1.1–1.5	80–85 (based on anode + cathode)	80% (Li^+) 74% (Zn^{2+}) 53% (Al^{3+}) 75% (Li^+/H^+), 1000, 5 $A.g^{-1}$	[73]

(*continued on next page*)

Table 2 (*continued*)

Dual-ion	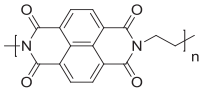 183.5	183.5	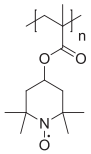 111	111		1 M $(NH_4)_2SO_{4\ (aq)}$	1.9	~2	136	86%,10,000, 5 A g^{-1}	[75]
Dual-ion	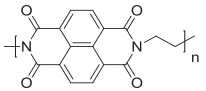 183.5	183.5	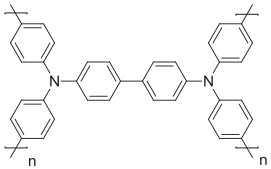 **109**	109		2 M LiTFSI in ethyl acetate (55 °C – 70 °C)	1.2	~1	69 (anode-limited, −70 °C)	-,-,-	[78]
Dual-ion	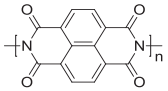 203	203	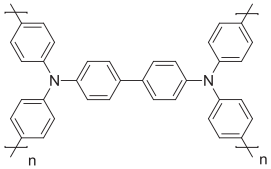 **111**	111		EMITFSI	1.5	0.7–2.0 (anode) 2.5–4.2 (cathode)	93	75%,5000,20C	[63]
Dual-ion	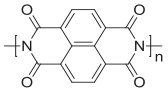 203	203	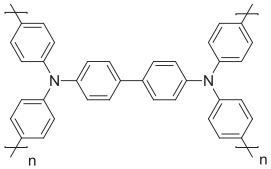 **111**	111		1 M EMITFSI in MA/ACN (1/2, v/v)	1.3	0.78 (anode) 1.3 (cathode)	108	86%,2000,5C	[79]
Dual-ion	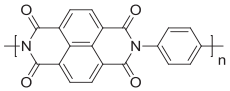 Nanofiber composite -	Nanofiber composite -	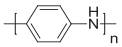 Nanofiber composite -	Nanofiber composite -		1 M $(NH_4)_2SO_{4\ (aq)}$	1.0	–	121	71%,2000, 1 A g^{-1}	[80]

[a] Theoretical capacity of each electrode, individually. The theoretical capacity of the limiting electrode in the full cell is indicated in bold.

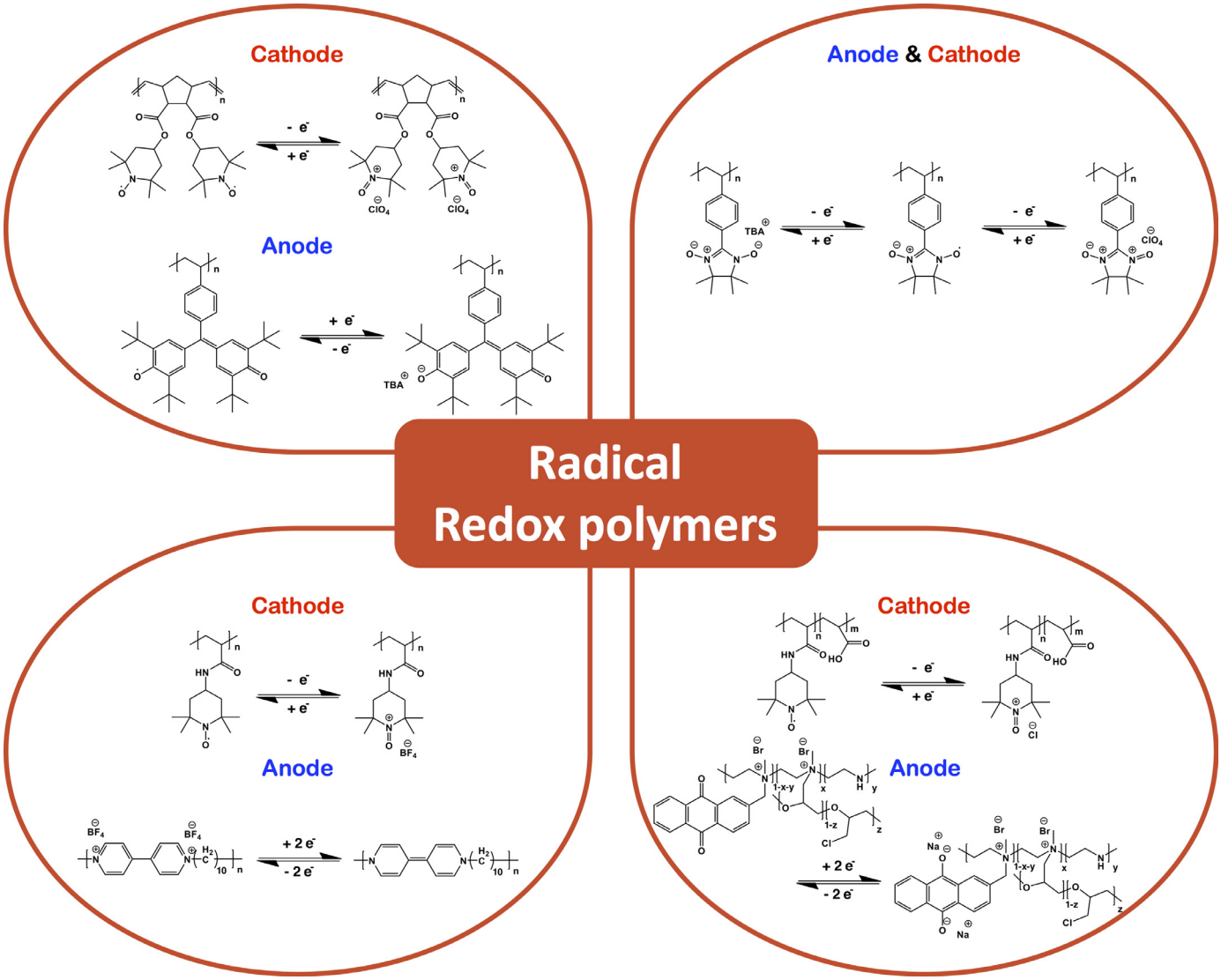

Fig. 9. Examples of all-polymer batteries using radical redox polymers: Top-left ([20]), Top-right ([35]), Bottom-left: ([83]) and Bottom-right ([84]).

cycles at a 60C rate. This difference in cycling stability was attributed to the low coulombic efficiency and inferior stability of the viologen-based redox polymer anode, PV10.

Schubert and co-workers, building on the initial work proposed by Nishide and co-workers on radical redox polymers, developed a novel anode material based on a poly(acetylene) with a (para-ethynylphenyl)hydrogalvinoxyl pendant group [86]. Using one of the most well-known radical redox polymer, poly(2,2,6,6-tetramethylpiperidine-N-oxyl)methacrylate polymer (PTMA) as a cathode material, an all-polymer battery was constructed using a benign and environmentally friendly sodium chloride aqueous electrolyte. However, this radical polymer battery delivered a discharge capacity of 27 mAh.g^{-1}, corresponding to only 50% of its theoretical capacity. Additionally, a low coulombic efficiency of 71% was observed. The poor cycling performance observed for this radical polymer battery was partly attributed to the incompatibility between the electrolyte and redox polymers. Indeed, PTMA was previously reported to work best under neutral or slightly acidic conditions, while galvinoxyl-based redox polymers performs best in basic electrolyte, highlighting the importance in finding an optimal electrolyte system for both organic electrodes.

In 2018, Nishide and co-workers reported of a fabrication method for redox polymer electrode, based on a self-assembled continuous conductive network of single-walled carbon nanotubes (SWCNTs) and poly(2,2,6,6-tetramethyl-piperidinyloxy-4-yl acrylamide) (PTAm), via a simple wetted grinding method [84]. (See Fig. 9) The continuous conductive network of SWCNTs enabled the fabrication of redox polymer electrode with high areal capacities (i.e. up to 3.3 mAh.cm^{-2}) due to the minimal amount of carbon additives required (i.e. 1–5 wt.%) to ensure sufficient electrical conduction throughout the entire electrode. Such high mass loading electrodes of sub-millimetre thickness, yet without compromising on their mechanical flexibility represents a significant improvement in the research field, corresponding to a 10-to-100-fold increase from the previous reports. The electrochemical performance of the PTAm/SWCNTs was first assessed in a half-cell configuration, delivering specific capacities of 90 mAh.g^{-1} and 78 mAh.g^{-1} under an applied C-rate of 10C for redox polymer electrodes with an areal capacity of 1.4 mAh.cm^{-2} and 3.3 mAh.cm^{-2}, repsectively. The 1.4 mAh.cm^{-2} PTAm/SWCNTs electrode displayed high rate capability, retaining 72% of its initial capacity, when increasing C-rate from 10C to 720C, with the latter corresponding to an unparalleled areal current density of 0.59 A.cm^{-2}. The authors employed again this hybridization method to prepare a redox polymer anode, based on poly(anthraquinone-substituted ethyleneimine) (PAQE), to construct an all-polymer battery. The re-

sulting PAQE||PTAm cell, with an areal capacity of 1.1 mAh.cm^{-2}, exhibited an average output voltage of 1.1 V. Moreover, when considering the high electrode loading level of this all-polymer battery, excellent long-term cycling stability was demonstrated, with 68% retention of its initial capacity upon 1000 cycles at a C-rate of 10C.

In their pursuit of ultrathin and stretchable all-polymer battery, Nishide and co-workers proposed another hybridisation method based on a conductive SWCNTs mesh material for the preparation of organic redox polymer electrode [87]. In the present method, hybridisation is performed using a dip coating method of redox polymer onto the SWCNTs mesh material, enabling electrode thickness in the order of 100 nm. The resulting PTAm/SWCNTs mesh electrode displayed high rate capability, delivering 98% of its theoretical capacity, even at a high C-rate of 430C (i.e. 0.4 mA.cm^{-2}). Using again the previously reported PAQE and PTAm redox polymers, the fabrication of a micrometre-thick all-polymer battery was demonstrated, yielding a specific discharge capacity of 80 mAh.g^{-1}, of which 90% remained after 40 cycles at a C-rate of 18C.

In 2020, Schubert and co-workers reported the development of a printable solid-state electrolyte for application in solid-state all-polymer battery [88]. This UV-cured electrolyte was based on methacrylate-based monomers (i.e. benzyl methacrylate and poly(ethylene glycol) methyl ether methacrylate), a cross-linker, a functional nano-filler and an ionic liquid. This printable electrolyte was then assessed in an all-polymer battery, consisting of a poly(2,2,6,6-tetramethyl-4-piperidinyl-N-oxyl methacrylate) (PTMA) and a poly(2-vinyl-11,11,12,12-tetracyano-9,10-anthraquinonedimethane) (poly(TCAQ)) as the cathode and anode, respectively. Despite a pre-wetting step the redox polymer electrodes with the pristine ionic liquid to ensure good contact, a low specific discharge capacity of 24 mAh.g^{-1} was still obtained, due to poor affinity between the ionic liquid and redox polymer electrodes.

Recently, Hatakeyama-sato et al. proposed a solid-state all-polymer battery, based on aliphatic polyether containing either TEMPO, viologen and imidazolium, for application as cathode, anode and electrolyte materials, respectively [89]. The resulting cell was able to deliver a specific capacity of 86 mAh.g^{-1} at a C-rate of 0.5C, which corresponds to 78% of its theoretical capacity at room temperature. Considering the use of a solid-state electrolyte, the cell displayed good capability, delivering specific capacities of 80 mAh.g^{-1} and 48 mAh.g^{-1}, at a C-rate of 1C and 5C, respectively. Unfortunately, the cell exhibited poor cycling stability, with only 79% capacity retention after 25 cycles.

Table 3 summarizes all all-polymer battery prototypes reported to date using radical redox polymers.

3.5. Miscellaneous redox polymers in all polymer batteries

Besides carbonyl and radical redox polymers, other redox-active functionalities, such as viologen, triphenylamine, thianthrene and phenothiazine, have also been investigated in all-polymer battery and some keys examples are illustrated in Fig. 10.

In 2013, a novel highly cross-linked poly(viologen) hydrogel, poly(tripyridiniomesitylene) (PTPM), was developed by Nishide and co-workers, for application in aqueous all-polymer batteries [30]. (See Fig. 10) The PTPM electrode showed superior cycling stability when compared to previously reported viologen-based redox polymer, which was attributed to the highly crosslinked network of the polymer, preventing dissolution into the electrolyte. As a result, 85% of the initial specific discharge capacity of 174 mAh.g^{-1} remained after 5000 cycles at a C-rate of 60C. The PTPM electrode also displayed excellent rate capability in a half-cell configuration, still delivering 150 mAh.g^{-1} at a very high C-rate of 1200C. Using the aforementioned PTAm polymer as cathode developed by the same group, an aqueous all-polymer battery was then constructed, employing an environmentally benign aqueous electrolyte based on sodium chloride. This anionic rocking-chair battery, anode-limited by design, displayed high rate capability, delivering 63% of its theoretical capacity at a very high C-rate of 1200C. Despite the improved cycling performance of the PTPM electrode, the long-term cycling stability of the PTPM||PTAm cell was similar to that of the previously reported PV10||PTAm cell [83,85], with ca. 80% capacity retention after 2000 cycles [30]. It is noteworthy that a larger water uptake during cycling was previously reported for PTAm electrode, when a $NaCl_{(aq)}$ electrolyte was used instead of $NaBF_{4(aq)}$, potentially promoting partial dissolution of the oxidized PTAm into the electrolyte, and thus, capacity fading [85]. This highlights the importance and difficulty in selecting the appropriate electrolyte system for both anode and cathode redox polymer electrodes in an all-polymer battery.

In the same year, another viologen based redox polymer was proposed by Sen et al., based on a covalently attached viologen pendant group to poly(pyrrole) backbone, pPy-V^{2+}-Me [92]. However, the pPy-V^{2+}-Me electrode displayed limited cycling stability in a half-cell configuration, with 30% capacity fading over 100 cycles. Nevertheless, an all-polymer battery was demonstrated using a poly(pyrrole) doped with 2,2′-azino-bis(3-ethylbenzothiazoline-6-sulfonic acid) (pPy[ABTS]), as cathode, yielding to an average output voltage of 1.2 V and similar cycling performance.

In 2015, Yao et al. reported an all-polymer battery, based on poly(1,1′-pentyl-4,4′-bipyridinium dihexafluorophosphate) (PVK) and poly(N-vinylcarbazole) (PBPy), as anode and cathode, respectively [93]. The anionic rocking-chair battery exhibited an average output voltage of 1.8 V, and delivered an initial specific discharge capacity of 100 mAh.g^{-1}, which corresponds to 96% of its theoretical capacity (i.e. anode-limited by design, 105 mAh.g^{-1}). However, the all-polymer battery exhibited poor cycling stability, with only 65% capacity retention after 100 cycles at a current density of 0.1 A.g^{-1}, due to dissolution of the PBPy anode into the electrolyte during cycling.

In 2017, Schubert and co-workers proposed an all-polymer battery, using two novel organic polymeric anode and cathode materials, based on 11,11,12,12-tetracyano-9,10-anthraquinonedimethane (TCAQ) and thianthrene redox-active groups, respectively, employing step-efficient synthesis methodologies [28]. The resulting all-polymer battery leds to a remarkably flat discharge voltage plateau of 1.35 V, delivering a specific discharge capacity of 105 mAh.g^{-1} at C-rate of 1C, which corresponds to 96% of the poly(2-vinylthianthrene) theoretical capacity. Unfortunately, a reasonable capacity fading was observed upon further cycling, retaining 67% of its initial capacity after 250 cycles.

In 2017, Dong et al. proposed a novel aqueous electrolyte, based on the “water-in-salt” concept [94], for application in all-polymer battery [29]. This “water-in-salt” electrolyte consisted of an 21 molal aqueous solution of lithium bis(trifluoromethanesulfonyl) imide salt (LiTFSI). The use of such high LiTFSI concentration has been previously reported to expand the electrochemical stability window of traditional aqueous electrolytes, based on salt-in-water concept, by pushing both cathodic and anodic potential limits related to hydrogen and oxygen evolution processes, respectively [94]. This expanded electrochemical stability window allows the use of high voltage redox polymer electrode materials, which was otherwise restricted to energy storage systems based on organic electrolytes. Taking advantage of this extended stability window, Dong et al. proposed the use of a high voltage organic cathode material based on poly(triphenylamine) (PTPAn) for application in aqueous all-polymer battery [29]. While the PTPAn electrode suffered from parasitic reactions related to oxygen evolution processes when using common neutral aqueous electrolytes, such

Table 3
Overview of all-polymer batteries based on radical redox polymers.

Cell type	Anode	Theoretical capacity ($mAh.g^{-1}$) [a]	Cathode	Theoretical capacity ($mAh.g^{-1}$) [a]	Electrolyte	Output voltage (V)	Active material loading ($mg.cm^{-2}$)	Specific capacity ($mAh.g^{-1}$)	Capacity retention, cycle numbers, rate or current density	Ref
Dual-ion	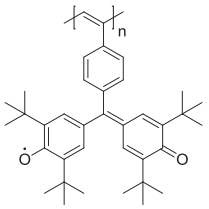 **51**	51	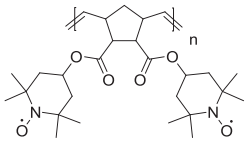 109	109	0.5 M n-Bu_4N ClO_4 + 0.01 M n-Bu_4NOH in ACN	0.66	–	32	74%,250,10C	[20]
Dual-ion	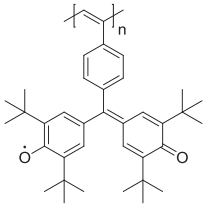 **51**	51	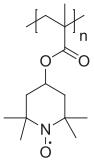 111	111	NaCl 0.1 M and 0.01 M n-Bu4NOH	~1.2	–	27	50%, 40 (anode only)	[86]
Anionic	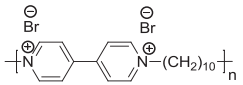 -	-	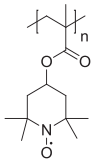 111	111	0.1 M $NaBF_4$	1.2	–	110 (anode-limited)	80%,2000, 60 C	[83]
Dual-ion	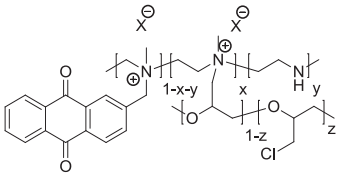 107	107	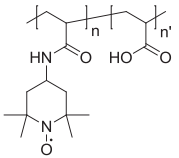 95	95	3 M NaCl	1.1	–	80	68%,1000,10C	[84]
Dual-ion	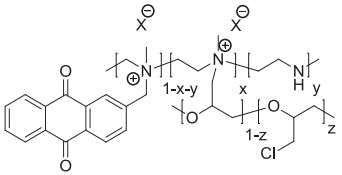 107	107	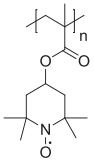 **111**	111	3 M NaCl	1.2	–	95	No loss, 60, 18 C	[87]

(*continued on next page*)

Table 3 (*continued*)

R_4N-ion	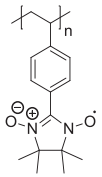	**103**	103	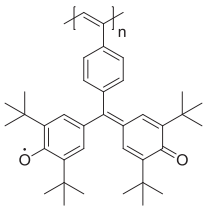	51	51	0.1 M n-Bu_4N ClO_4 + 0.01 M n-Bu_4NOH in ACN	0.6	–	29*	91%,250,150 C	[35]
Dual-ion	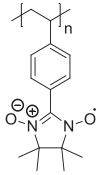	103	103	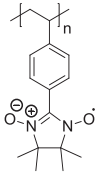	103	103	0.1 M n-Bu_4N ClO_4 + 0.01 M n-Bu_4NOH in ACN	1.33	–	44*	66%,250,60 C	[35]
Dual-ion	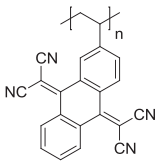	-	-	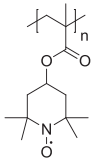	**111**	111	Vol IL:vol M 2:1, CQ-initiated, 10 mol% TEGDMA,	1V	1.5–2.7 mg (cathode) 3.8–5.7 mg (anode)	24	77,1000,1 C	[88]
Anionic	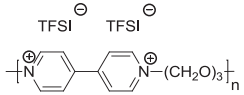	69	69	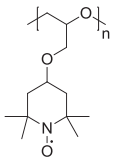	**107**	107	Vol IL:vol M 2:1, CQ-initiated, 10 mol% TEGDMA,  	1–1.6	–	80	79%,25,1C	[89]

[a] Theoretical capacity of each electrode, individually. The theoretical capacity of the limiting electrode in the full cell is indicated in bold.*Specific capacity based on the total weight of active polymer in both anode and cathode electrodes.

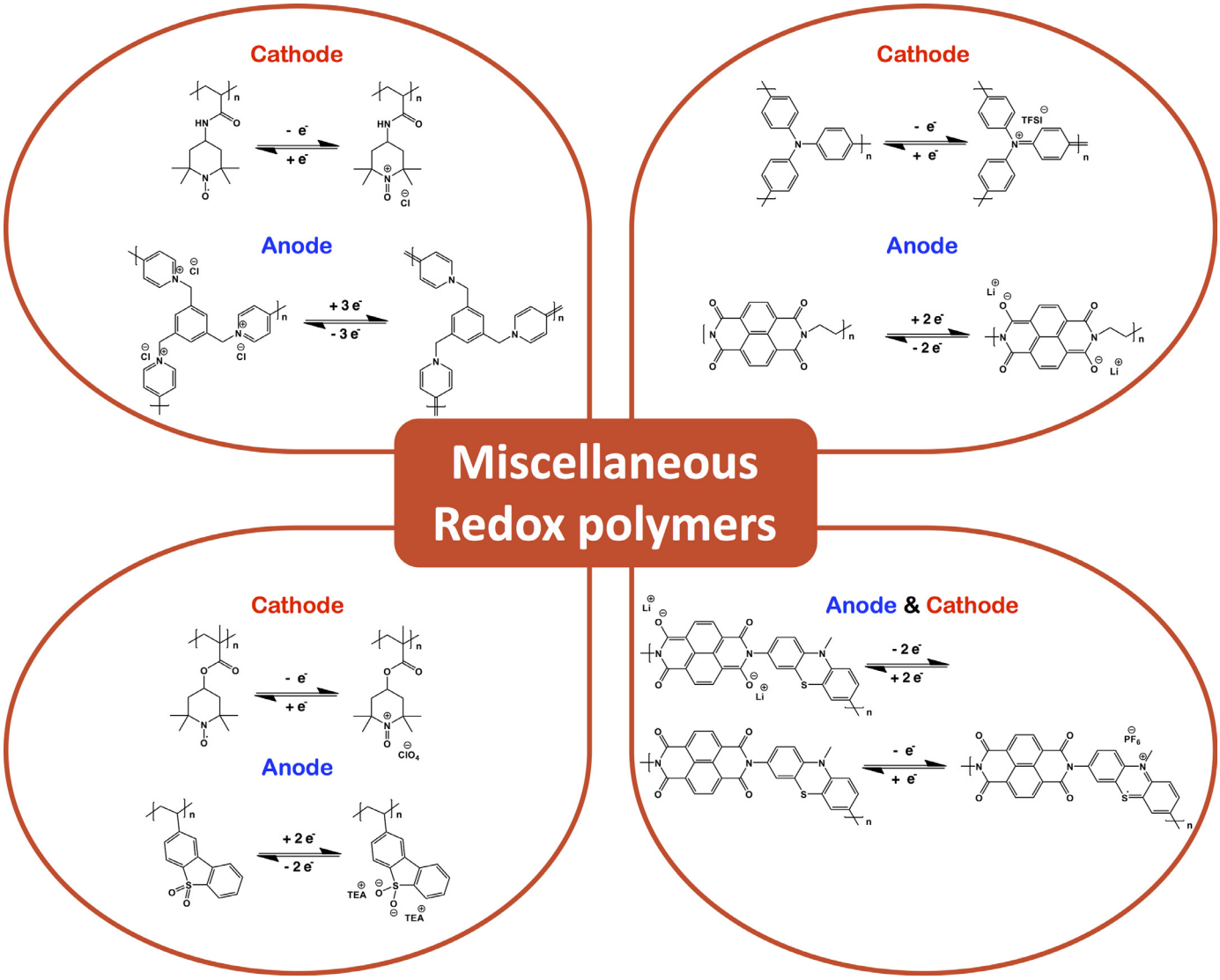

Fig. 10. Examples of all-polymer batteries using on miscellaneous redox polymers: Top-left ([30]), Top-right ([29]), Bottom-left: ([90]) and Bottom-right ([91]).

as 1 M lithium sulphate, 2 M lithium nitrate, 2 M lithium perchlorate, and 2 M lithium acetate. However, in the "water-in-salt" electrolyte, the PTPAn exhibited characteristic redox behaviour, featuring two pairs of reversible redox peaks centred at a potential of 0.2 V and 0.6 V (vs. SCE), with coulombic efficiency approaching 100%. Using a poly(1,4,5,8-naphthalenetetracarboxylic bisimide) anode in conjunction with the PTPAn cathode, all-polymer battery, based on the so-called "water-in-salt" electrolyte, was constructed. This dual-ion polymer cell was able to deliver 96% of its theoretical capacity (i.e. cathode-limited by design), of which 85% remained after 700 cycles at a C-rate of 1C. High rate capability of the device was also demonstrated, still delivering 70% of its initial capacity, when increasing the applied current density from 0.5 $A.g^{-1}$ to 10 $A.g^{-1}$. Such results demonstrated the importance of the electrolyte composition on the performance of high energy density all-polymer batteries based on aqueous electrolyte.

In 2018, an redox polymer anode material based on poly(vinyldibenzothiophenesulfone) was proposed by Nishide and co-workers for application in all-polymer batteries [90]. (See Fig. 10) This redox polymer anode revealed a two-electron reduction reaction at a potential as low as −1.8 V (vs. Ag/AgCl), allowing for higher energy density all-polymer batteries. The poly(vinyldibenzothiophenesulfone) anode displayed a good cycling stability, delivering an initial specific discharge capacity of 211 $mAh.g^{-1}$ with only 5% capacity fading upon 100 cycles. When coupled with the well-known poly(TEMPO substituted methacrylate) (PTMA), Nishide and co-workers proposed an all-polymer battery, which yielded to an average output voltage of 2.6 V, resulting in one of the highest specific energy density of 541 $Wh.kg^{-1}$ with respect to the mass of the anode active material only, for an all-polymer battery.

Recently, Casado et al. proposed an alternative approach, via synthesizing a dual redox-active polyimide copolymer, composed of phenothiazine and naphthlene moieties, for application in all-polymer battery [91]. (See Fig. 10) It is worth to mention that this dual redox-active copolymer can be used as both cathode and anode, with no additional prelithiation step required for the latter. The resulting symmetric polymer battery can be charged up to a voltage of 1.7, exhibiting a rather sloping (dis-)charge curves. Although, a low coulombic efficiency was observed at low current density (i.e. $\leq$ 200 $mA.g^{-1}$), the symmetric polymer battery exhibited high rate capability, with no discharge capacity decay (i.e. 124 $mAh.g^{-1}$), when increasing current densities from 50 $mA.g^{-1}$ to 1000 $mA.g^{-1}$. Additionally, excellent long-term cycling stability was also demonstrated with 94% capacity retention after 1000 cycles.

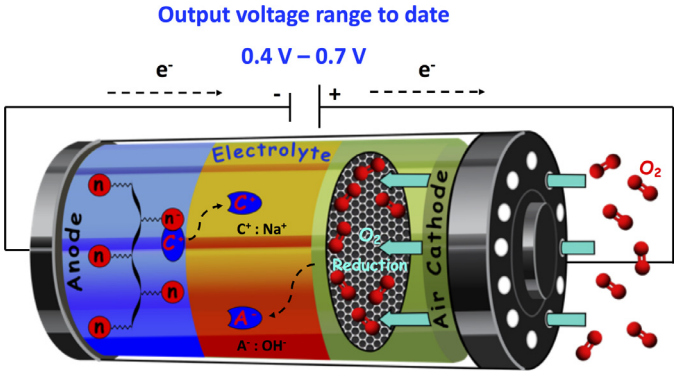

Fig. 11. Schematic illustration of redox polymer-air battery, based on a basic aqueous electrolyte and a n-type redox polymer is used as anode.

Table 4 summarizes all-polymer battery prototypes reported to date using miscellaneous redox polymers.

4. Polymer-air batteries

4.1. Introduction

Metal-air rechargeable batteries have attracted a lot attention due their high theoretical energy density, as a promising battery technology as a substitute to the current Li-ion battery, especially for electric vehicles and grid-scale energy storage applications [95–97]. Among all the metal-air chemistries investigated, rechargeable lithium-air and Zinc-air battery technologies are the most studied and advanced in their development [95–97]. However, these air battery technologies are still facing challenges, prior becoming a commercial reality, related with the cycling stability of either the air-cathode or the metal anode. With respect to the latter, redox polymers have been recently proposed as promising substitutes to the highly reactive metal anodes, addressing safety and cycling stability concerns, as highlighted in Fig. 11. [98]. The use of redox polymers as anode materials in air rechargeable batteries appears as a promising solution, especially with the recent development in redox polymer electrode engineering, enabling high areal capacity redox electrode (i.e. ~ 6 mAh.cm^{-2}) [99].

4.2. Examples of polymer-air batteries

Redox polymer-air battery is a recent technology, with only limited prototypes reported to date, all based on aqueous electrolytes as illustrated in Fig. 12. In 2011, Nishide and co-workers described the first known prototype of aqueous redox polymer-air battery, based on poly(vinylanthraquinone) (PVAQ) anode [98]. (See Fig. 12) The electrochemical performance of PVAQ electrode was first investigated in a typical aqueous electrolyte used for alkali-metal-air battery (i.e. 30 wt.% NaOH), in a three-electrode configuration. The PVAQ electrode displayed good redox activity and delivered 94% of its theoretical capacity, of which 91% remained after 300 cycles. Using a conventional MnO_2/C air cathode, a redox polymer-air battery was then constructed, yielding to an average output discharge voltage of 0.5 V. The resulting polymer-air battery was able to deliver an initial specific discharge capacity of 214 mAh.g^{-1}, even at high current density of 34 A.g^{-1} (i.e. 150C rate). This first prototype displayed moderate cycling stability with 69% capacity retention after 500 cycles.

Later on, Nishide and co-workers proposed an optimized version of their polymer-air battery, through the design of a more robust and stable poly(dianthraquinone-substituted norbornene) (PQNB), limiting the elution issues in basic aqueous electrolyte associated during the reduction of anthraquinone moiety, due to the more pronounce hydrophobic character of the norbornene polymer backbone [100]. This resulting polymer-air battery exhibited improved cycling stability with 96% capacity retention upon 300 cycles. In 2019, Li et al. proposed a poly(1,4-anthrquinone)/carbon nanotube composite electrode, via in situ polymerization, for application in polymer-air battery [101]. The resulting polymer-air battery exhibited high rate capability, delivering 58% of its initial capacity (i.e. 147 mAh.g^{-1}) when current density was increased from 0.2 to 10 A.g^{-1}. Additionally, excellent long-term cycling stability of the device was also demonstrated, with 98 % capacity retention after 500 cycle at a current density of 1 A.g^{-1}. Recently, Sjödin and co-workers developed a novel conducing redox polymer (pEP(NQ)E), based on poly(3,4-ethylenedioxythiophene and naphthoquinone as polymer backbone and pendant group, respectively, for application in aqueous polymer-air batteries [102]. (See Fig. 12) The resulting polymer-air battery exhibited good rate capability, retained 74% of its theoretical capacity even at an elevated C-rate of 45C. The cycling stability of the battery was also assessed, retaining 98% of its initial capacity over 100 cycles at a C-rate of 5C. In 2020, Nishide and co-workers developed another naphthoquinone based redox polymer, via partial substitution a poly(allyamine) polymer by naphthoquinone moieties (i.e. PNQ, 28%), for application in aqueous polymer-air batteries [103]. The PNQ electrode exhibited good cycling stability with 99% capacity retention after 100 cycles, as well as good rate capability with 83% of theoretical capacity achieved even at an elevated C-rate of 60 C. A polymer-air battery prototype was assembled using the PNQ electrode and a Pt/C electrode, as anode and cathode, respectively. The polymer-air battery showed similar performance than that of the PNQ electrode, with 93% capacity retention after 100 cycles at a C-rate of 15 C and 76% capacity retention when C-rate was increase from 10 C to 60 C.

Table 5 summarizes all redox polymer-air battery prototypes reported to date.

5. Polymer redox flow batteries (pRFB)

5.1. Introduction

In previous sections, redox-polymers were employed as active materials mixed with additional additives (carbons as conductivity enhancer and polymer binder) to get solid electrodes generally stuck to metal foil current collectors. Recently, redox-polymers have been also employed as soluble active materials to develop redox electrolytes with application in polymer redox flow batteries (pRFB) (see Fig. 13) [104].

In fact, one of the most promising approaches for the replacement of the problematic vanadium compounds, currently used as active material in RFB, is their substitution by organic redox-active molecules, which are cost-efficient, abundant, and environmentally friendly. In recent years, TEMPO-, viologen-, and quinone-derivatives have proven to be the most suitable redox small organic molecules for application in aqueous RFBs due to a good long-term cycling stability (> 1000 charge/discharge cycles), high coulombic efficiencies (> 98%), and energy densities up to 10 Wh/L. The main advantage of using redox polymers instead of redox-active small organic molecules in RBF is that, in principle, due to the big size of macromolecules it is possible to substitute the inefficient and expensive ion-selective membrane, necessary to keep the two electrolytes separated avoiding cross-over or cross-contamination, by cheaper size-exclusion membranes that still allow small ions to pass as charge carriers (see Fig. 13).

However, redox polymers suffer from low solubilities compared to small-molecules which limits the volumetric capacity of pRFBs. Therefore, differently from conventional “static” batteries where insoluble polymers are aimed to guarantee long cyclabil-

Table 4
Overview of all-polymer batteries based on miscellaneous redox polymers.

Cell type	Anode	Theoretical capacity (mAh.g^{-1}) [a]	Cathode	Theoretical capacity (mAh.g^{-1}) [a]	Electrolyte	Output voltage (V)	Active material loading (mg.cm^{-2})	Specific capacity (mAh.g^{-1})	Capacity retention, cycle numbers, rate or current density	Ref
Anionic	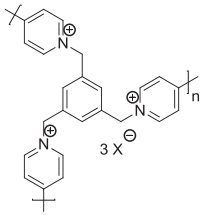	**175** 175	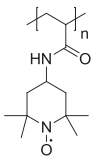	114 114	0.1 M NaCl	1.1–1.5	–	110	80%,2000,60C	[30]
Anionic	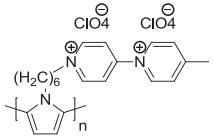	68 68	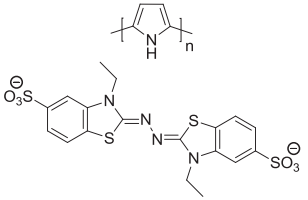	22 22	0.2 M $LiClO_4$ in CH_3CN	1	–	16	70%,100, 0.5 mA/cm^2	[92]
Anionic	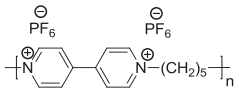	104 104	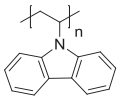	**139** 139	1 M $TBAPF_6$ in PC	1.8	2 mg (cathode) 8 mg (anode)	100	65%,100, 0.1 A.g^{-1}	[93]
Dual-ion	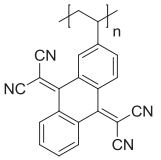	138.4 138.4	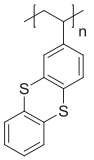	**110.6** 110.6	1 M $LiClO_4$ in EC:DMC 3:7 (v/v)	1.35	–	105	67%,250,1C	[28]

(*continued on next page*)

Table 4 (*continued*)

Dual-ion	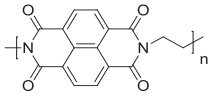 183.5	183.5	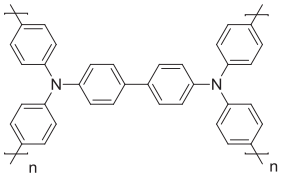 **109**	109	LiTFSI 21 M (pH 7)	~0.6	~1	105 (cathode-limited)	85%,700, 1 C	[29]
Dual-ion	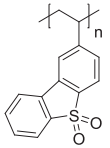 **221**	221	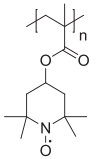 111	111	1 M Et_4NClO_4 in ACN	2.6	–	208 (Anode, half-cell)	95%, 100, 120C	[90]
Dual-ion	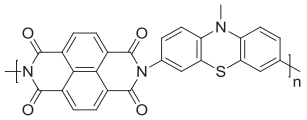 169.3	169.3	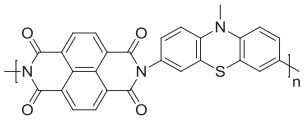 **169.3**	169.3	1 M $LiPF_6$ in EC/DMC	1.2	~1	77	94,1000,800 mAg^{-1}	[91]

[a] Theoretical capacity of each electrode, individually. The theoretical capacity of the limiting electrode in the full cell is indicated in bold.

Table 5
Overview of redox polymer-air batteries.

Cell type	Anode	Theoretical capacity ($mAh.g^{-1}$) [a]	Cathode	Theoretical capacity ($mAh.g^{-1}$) [a]	Electrolyte	Output voltage (V)	Active material loading ($mg.cm^{-2}$)	Specific capacity ($mAh.g^{-1}$)	Capacity retention, cycle numbers, rate or current density	Ref
Dual-ion	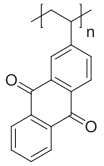 **229**	229	O_2		NaOH 30 wt.%	0.7–0.4	–	214	69%,500,150C	[98]
Dual-ion	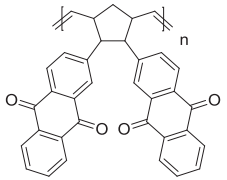 **212**	212	O_2		10 M $NaOH_{(aq)}$	0.7	–	205	96%,300,-	[100]
Dual-ion	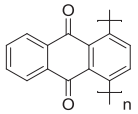 **260**	260	O_2		6 M KOH	0.7	~2	147	95%,100, 1 Ag^{-1}	[101]
Cationic	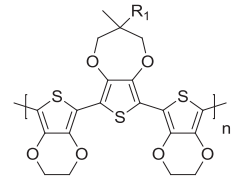 **76**	76	O_2		$H_2SO_{4(aq)}$ (pH 1)	0.5	2	76	98%,100,5C	[102]
Cationic	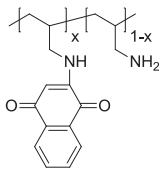 **124**	124	O_2		0.5 M $H_2SO_{4(aq)}$	0.8	–	124	93%,100, 15C	[103]

[a] Theoretical capacity of each electrode, individually. The theoretical capacity of the limiting electrode in the full cell is indicated in bold.

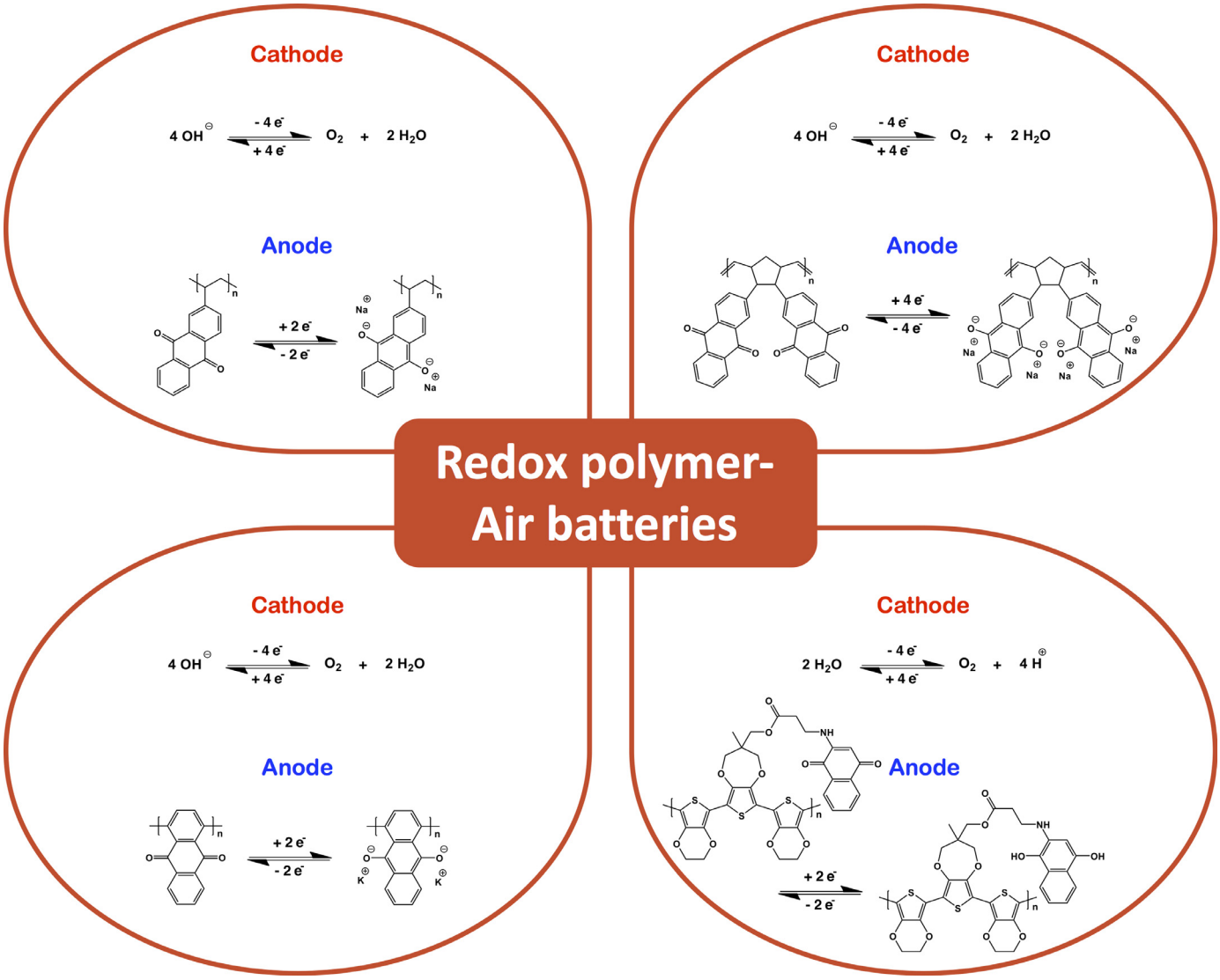

Fig. 12. Examples of redox polymer-air batteries: Top-left ([98]), Top-right ([100]), Bottom-left: ([101]) and Bottom-right ([102]).

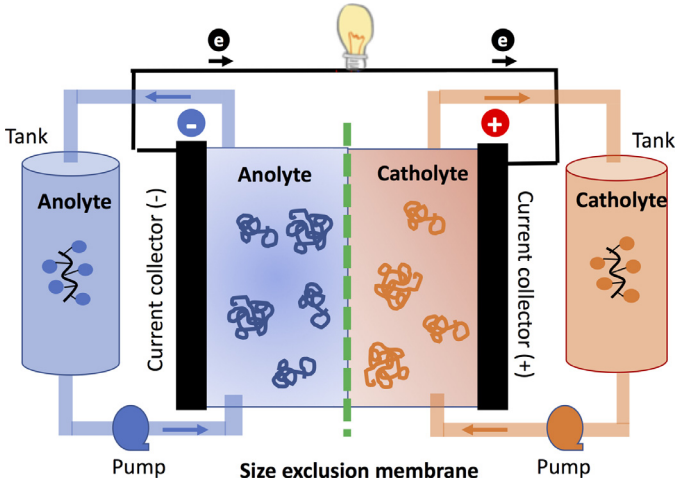

Fig. 13. Schematic illustration of polymer-based Redox Flow Batteries (pRFB) with polymer solutions, polymeric colloidal dispersions or suspensions of polymer particles as active species in both anolyte and catholyte. Ion-selective membranes are substituted here by cheaper size exclusion membranes.

ity, redox polymers employed in pRFB should be specifically designed to have high solubilities since energy density depends on both specific capacity of the redox polymer and its concentration in the electrolyte. Unfortunately, most synthetic strategies explored to increase the solubility of redox polymers in the electrolyte rely on the incorporation of large functional groups that ultimately decrease the specific capacity of the polymers. It is necessary, therefore, to find an optimum trade-off between solubility and specific capacity to achieve pRFBs with adequate electrochemical metrics. Another disadvantage of pRFB is that the viscosity of the redox electrolytes significantly increases with the concentration of polymer which eventually causes a serious penalty in the electrolyte transport properties and a relevant increase in pumping electrolyte cost. In this sense, an interesting approach is to use the redox-active compounds not dissolved in solution but in form of micelles, colloids, or microparticles. Here, an overview of the different soluble redox structures employed in aqueous and non-aqueous pRFB will be presented. More sophisticated polymer architectures forming micellar or dispersion-based pRFB will be also presented and discussed. Most relevant examples are included in Table 6 and Fig. 14.

Table 6
Overview of all polymer Redox Flow batteries (pRFB) including soluble polymers, colloids and dispersions.

Cell type	Anolyte (Concentration)	Catholyte (Concentration)	Electrolyte	Separator	Cell voltage (V)	Capacity retention, cycle numbers, rate or current density	Energy desnity (Wh.L $^{-1}$)	Ref
Conventional RFBs with soluble polymer species								
Anionic	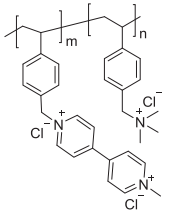 10 Ah.l^{-1} 10 Ah.l^{-1}	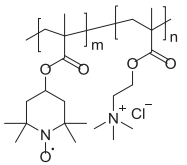 10 Ah.l^{-1} 10 Ah.l^{-1}	2 M NaCl	Cellulose dialysis membrane (molecular weight cut-off 6000 – 8000 g mol^{-1})	1.1	78%, ~105, 40 mA.cm^{-2}	10.8 (charging) 8.0 (discharging)	[105]
Anionic	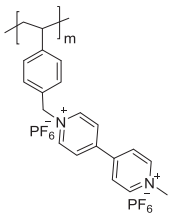 0.01 M 0.01 M	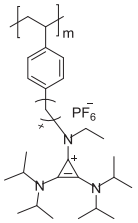 0.01 M 0.01 M	0.1 M $TBAPF_6$ in MeCN					
	Celgard 2400 coated with size excluding cross- linked PIM-1	1.55	20%, 10, 0.6	N.A.				[114]
Dual-ion	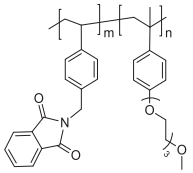 0.01 M 0.01 M	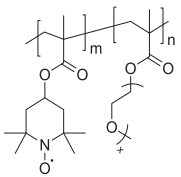 0.01 M 0.01 M	0.5 M NBu_4ClO_4 in DMF					
	Celgard 3419s	2.2	60%, 10, 0.5 mA.cm^{-2}	N.A.*				[106]
Dual-ion	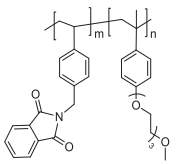 0.01 M 0.01 M	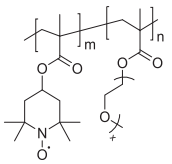 0.01 M 0.01 M	0.5 M LiTFSI in DME					
	Celgard 3419s	2.0	60%, 10, 0.4 mA.cm^{-2}	N.A.*				[106]

(*continued on next page*)

Table 6 (*continued*)

Dual-ion	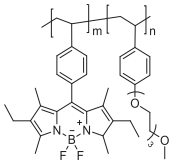 0.006 Ah.l^{-1}	0.006 Ah.l^{-1}	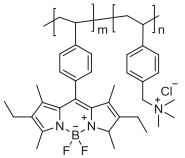 0.006 Ah.l^{-1}	0.006 Ah.l^{-1}	0.5 M Bu_4NClO_4 in PC					
	Cellulose dialysis membrane (molecular weight cut-off 1000 g mol^{-1})		1.67		60%, 100, 0.025 mA	0.5*	[107]			
Dual-ion	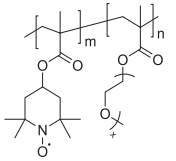 0.06 Ah.l^{-1}	0.06 Ah.l^{-1}	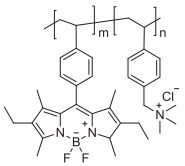 0.06 Ah.l^{-1}	0.06 Ah.l^{-1}	0.5 M Bu_4NClO_4 in PC	Cellulose dialysis membrane (molecular weight cut-off 1000 g mol^{-1})	1.93	70%, 100, 0.25 mA	0.5*	[107]
RFBs with insoluble polymer species (polymer particles, colloids, suspensions)										
Dual-ion	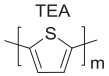 0.1 eq. M	0.1 eq. M	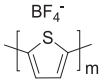 0.1 eq. M	0.1 eq. M	1 M $TEABF_4$ in PC (with 2 g/l Ketjen-black)					
	Fumasep® FAP-PP-375		1–3 (sloping)		84%, 10, 0.5 mA.cm^{-2}	N.A.	[116]			
Anionic	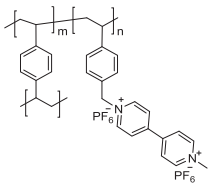 0.01 M	0.01 M	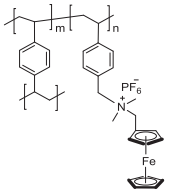 0.01 M	0.01 M	0.1 M $LiBF_4$ in MeCN					
	Celgard 2325		0.9		90%, 12, 0.04 mA.cm^{-2}	N.A.	[117]			

(*continued on next page*)

Table 6 (*continued*)

Anionic	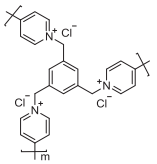 0.66 M	0.66 M	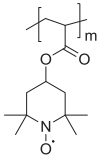 0.4 M	0.4 M	3 M NaCl	Cellulose dialysis membrane (pore size of 5 nm)	1.1	95%, 100, 1.5 mA.cm^{-2}	12.1	[118]
Dual-ion	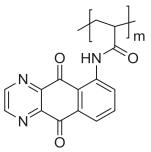 1.5 M	1.5 M	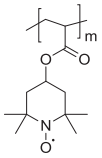 1.5 M	1.5 M	3 M NaCl	Cellulose dialysis membrane (pore size of 5 nm)	1.3	95%, 50, 4 mA.cm^{-2}	7.8	[118]
Cationic	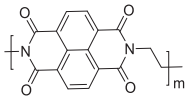 1.0 M	1.0 M	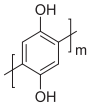 1.0 M	1.0 M	2 M H_2SO_4	Cellulose dialysis membrane (molecular weight cut-off 1000 g mol^{-1})	0.53	70%, 300, 20 mA.cm^{-2}	1.98	[108]
Cationic	Cationic 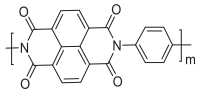 1.0 M	1.0 M	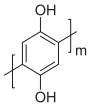 1.0 M	1.0 M	2 M H_2SO_4	Cellulose dialysis membrane (molecular weight cut-off 1000 g mol^{-1})	0.7	47%, 50, 5 mA.cm^{-2}	3.69	[108]

*static mode of operation.

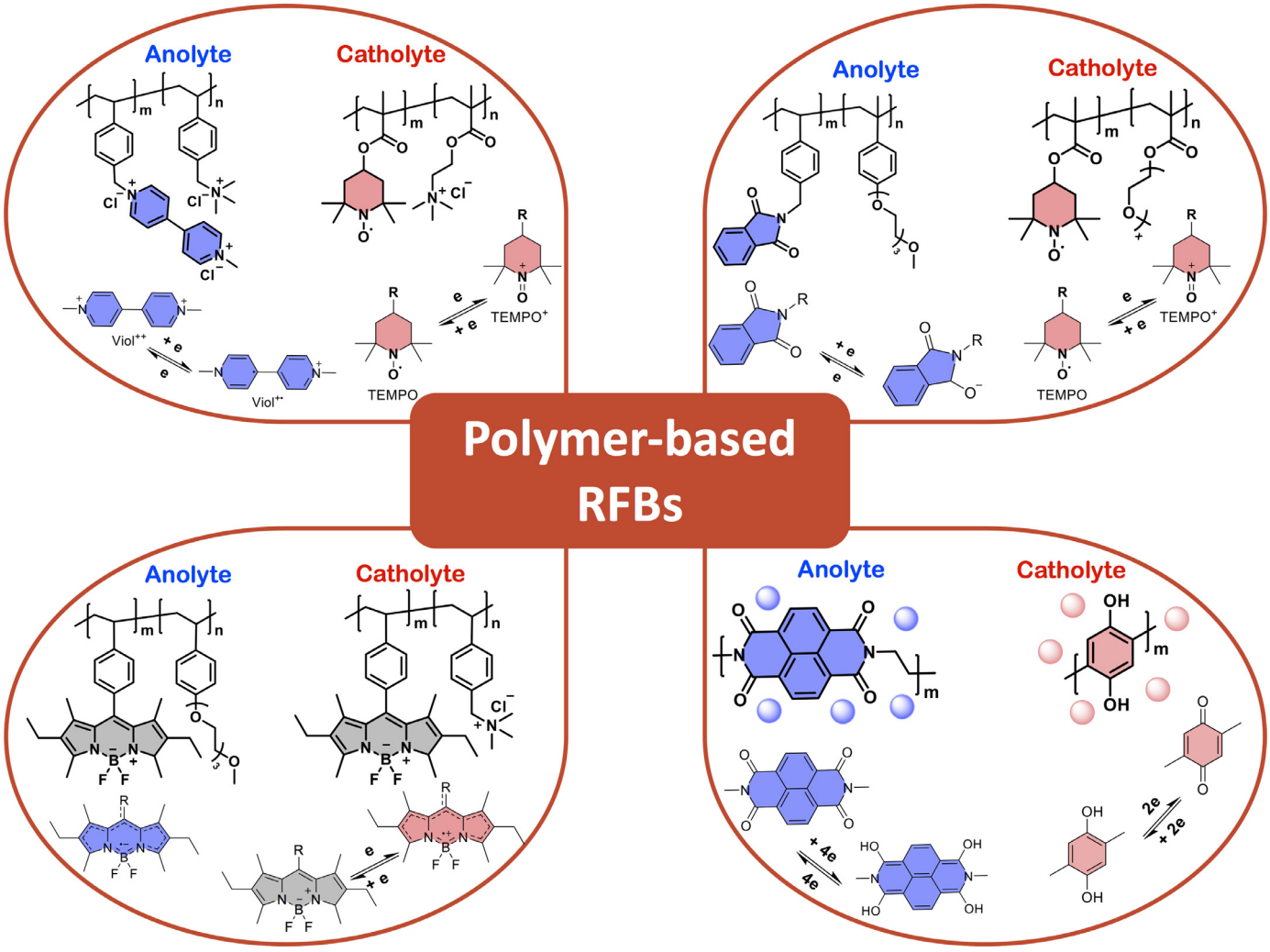

Fig. 14. Examples of polymer-based Redox Flow Batteries (pRFB). Top-left: aqueous pRFB ([105]), Top-right non-aqueous pRFB ([106]), Bottom-left: symmetric Bodipy-based pRFB ([107]) and Bottom-right: particulated pRFB ([108]).

5.2. Examples of polymer redox flow batteries (pRFB)

5.2.1. Aqueous pRFB

Although several articles anticipated the appropriate electrochemical properties of redox polymers in solution (mainly conducting polymers such as PEDOT and PANI) already in the 90′s, it was only in recent years, with the blooming of organic RFB research topic, when redox polymers were considered for RFB application. In 2015, Schubert et al. were the first to develop an aqueous, all-polymer-based RFB using a cost-efficient size-exclusion membrane instead of expensive ion-exchange membranes [105]. Copolymers of poly(viologen) and poly(TEMPO) both having non redox-active polycationic comonomer pendants to increase the solubility of polymers in the electrolyte, were synthesized using traditional radical polymerization (see Top-left Fig. 14). Moreover, both redox electrolytes were based on sodium chloride (2 M) in a pH-neutral aqueous medium which minimised the environmental impact, leading to a “green”, safe, non-corrosive, and low-cost energy storage system. The capacity of the pRFB reached 8.2 Ah/L with 82% material utilization at the current density of 40 mA/cm^2, corresponding to energy density of 10.8 Wh/l (charging) and 8.0 Wh/l (discharging) with a cell voltage of 1.1 V (see Table 6). The long-term cyclability experiments revealed a 75% capacity retention after 100 cycles. Further attempts to increase the solubility of poly(TEMPO) catholyte were developed by substituting the polycation copolymer segment (trimethylammonium chloride) by amphiphilic polyethylene glycol comonomer[109] or more recently by zwitterionic sulfopropylammonium copolymer segment [110]. The capacity of the zwitterionic poly(TEMPO) copolymer is over 20 Ah/L, which is the highest value reported for polymer redox-active materials in an aqueous system keeping reasonable values of viscosity. These new TEMPO copolymers were tested as catholytes in semi-pRFB using Zn foil as anode and combined with methyl viologen (MV) anolyte in RFB, respectively. However, their combination with polymer-based anolyte in a fully polymeric RFB has not been reported so far.

5.2.2. Non-aqueous pRFB

A recent strategy to boost the energy density of RFBs is to employ non-aqueous electrolytes with wider electrochemical window allowing higher voltage cell and consequently higher energy density. This strategy was initially explored with metal complexes but it was more successful with small organic molecules whose redox potential and solubility could be easily “adjustable” by chemical modification. However, the use of ion selective membranes in non-aqueous electrolytes is even more problematic than for aqueous systems. It is important to note that most ion selective membranes such as Nafion, have been specifically designed to operate in aqueous electrolytes while their performance in non-aqueous

electrolytes is hindered by their poor selectivity towards active species and by their insufficient ion conductivity in non-aqueous electrolytes. Therefore, the substitution of these membranes by size-exclusion membranes presenting both lower cost and better transport of supporting electrolyte is highly beneficial and might be achieved by substituting small redox molecules by larger compounds such as redox-polymers.

As summarized in Table 6, different polymers such as TEMPO-based polymer, viologen-based polymer, poly(ionic liquid), etc. were studied in non-aqueous RFB. Most representative examples are discussed in next sub-sections.

Viologen-based polymers: The group of Prof. Rodriquez-Rodriguez investigated the electrochemical properties of several poly(vinylbenzylethyl viologens) having different molecular weights (and consequently different size) in acetonitrile-based electrolyte where they all presented high solubility (up to 2 M). Besides solubility or viscosity, the transport properties across commercial separators such as CELGARD was systematically investigated demonstrating that the selectivity of those separators for charge balancing ions ($Li^+$and BF_4^-) compared to redox-active polymer increased with polymer molecular weight and reduction in separator membrane size [111]. A second generation of viologen polymers with a dimer structure was also investigated employing a bottom-up approach for evaluating the impact of structural and electronic effects on the electrochemistry of redox polymers in solution. It was demonstrated that if the two viologens units are located in the meta position the resultant polymer is electrochemically stable, presents faster kinetic and the number of redox pendants per unit are doubled compared to the first generation of poly(vinylbenzylethyl viologens) [112]. The size-exclusion efficiency of non-aqueous RFBs based on poly(vinylbenzylethyl viologens) was validated using an organometallic ferrocene-based polymer as the catholyte [113]. High Coulombic efficiencies above 98% and access up to 80% of capacity utilization were observed while lower overpotential and higher energy efficiencies were obtained with inexpensive nano-porous separators in comparison with ion selective membranes. Poly(vinylbenzylethyl viologen) anolyte was also combined with a cyclopropenium-containing redox polymer as a catholyte in a non-aqueous pRFB [114]. Although the voltage of the battery was as high as 1.55 V, the low concentration of active species (10 mmol) and the poor cycling performance (80% of the initial capacity was lost after 10 cycles) limited the applicability of this pRFB (see Table 6) [114].

TEMPO-based polymer: A TEMPO-based copolymer, poly(norbornene)-graft-poly(4-methacryloyloxy-2,2,6,6-tetramethylpiperidin-1-oxyl) (PNB-g-PTMA) having a bottlebrush structure was synthesized in 2014 by Prof. Nishide group and tested in a non-aqueous half-cell RFB envisaging the application of redox radical polymers in pRFB [115]. Capacity utilization was as high as 95% and the well-defined molecular dimension of the bottlebrush polymer was successfully retained in the porous separator. Prof. Schubert group also explored the application of TEMPO-based copolymers in non-aqueous systems by designing poly(TEMPO-co-PEGMA)s copolymers that were soluble in non-aqueous electrolytes due to the amphiphilic character of PEGDA group. These poly(TEMPO-co-PEGMA)s copolymers were tested as catholytes in semi-pRFB using Zn foil as anode, a size-exclusion membrane as separator and using a 0.1 M solution of $Zn(ClO_4)_2$ in EC/DMC/DEC (1:1:1) as electrolyte [109]. The capacity utilization was close to 100% at low current densities showing the excellent electrochemical participation of TEMPO redox moieties. The higher capacity (6.1 Ah/L) catholyte was achieved using a polymer with a high TEMPO ratio although lower capacity catholyte (0.91 Ah/L) was employed for cyclability test in a static cell configuration obtaining 81% capacity retention for 500 cycles.

In a further work, poly(TEMPO-co-PEGMA) catholyte was combined with a new phthalimide-containing redox-active polymer as anolyte in an all-polymeric non-aqueous RFB system with a high cell voltage (2 and 2.2 V in Li- and NBu_4-based electrolytes, respectively) (see Top-right Fig. 14) [106]. Despite of the excellent electrochemical properties of the poly(phthalimide)-based anolyte in CV, the battery exhibited a rapid capacity decay upon cycling (40% in 10 cycles under static conditions).

Symmetric pRFB based on BODIPY: One interesting example of non-aqueous pRFB was reported by Schubert et al. using a redox polymers bearing ambipolar BODIPY redox-active moieties both as anolyte and catholyte (see Bottom-left Fig. 14) [107]. BODIPY redox-moiety presents three redox states and is able to undergo two reversible redox reactions at separated redox potential (−1.5 and 0.7 V vs Ag/Ag^+) making it an excellent candidate for a symmetric design. This strategy mimics the all-vanadium RFB mitigating the irreversible long-term capacity decay by cross contamination while affects only the Coulombic efficiency. Following a similar strategy that in previous articles, polar comonomer groups were incorporated to the redox-polymer during the free radical polymerization to promote their solubility in non-aqueous electrolytes. An all-BODIPY static cell with two different BODIPY copolymers as anolyte and catholyte in a supporting electrolyte of 0.5 M Bu_4NClO_4 in propylene carbonate was fabricated with a size-exclusion membrane and tested. The cell had a charging plateau at 2.06 V and a sloppy discharging plateau at an average voltage of 1.28 V. Moreover, a sharp capacity decrease was observed in the first 10 cycles, while the subsequent 90 cycles were relative stable. The high overpotential observed between charge and discharge and the low coulombic efficiency (<90%) explained the lower energy efficiency in comparison with another pRFB in which the BODIPY catholyte was substituted by a poly (TEMPO-co-PEGMA) which exhibited a steady discharge voltage of 1.82 V, 99% coulombic efficiency and capacity fading of 30% after 100 cycles [107]. Although the assembled battery cannot be considered strictly symmetric (same bipolar copolymer in both electrolytes was not demonstrated) and it was tested only in static conditions, this work anticipated the use of redox-polymers in symmetric pRFB.

5.2.3. Polymer colloids- and nano(or micro)particle dispersions

The low electrochemical performance (specially in terms of energy density) of pRFB is mainly attributed to the low solubility of redox polymers and the high viscosity of polymer electrolytes. One recent strategy to overcome these issues is the development of polymer suspensions where the redox-polymers remain insoluble but forming a stable flowable electrolyte. Oh et al. presented the first attempt using a polythiophene-particle-based symmetric pRFB in 1 M $TEABF_4$ propylene carbonate electrolyte [116]. The conjugated nature of redox-polymer led to sloppy cell voltages, ranging from 1 to 3 V, resembling the electrochemical response of a supercapacitor. Moreover, low capacity utilization ratio of 35% was obtained likely due to the low conductivity of polythiophene polymer in the neutral state that hinder the redox conversion of the internal part of the big polymer particles. The pRFB was tested under flowing conditions during 30 cycles exhibiting a stable electrochemical performance and demonstrating the principle proof of concept of suspension-based pRFB.

Then, in 2016 Rodríguez-López et al. reported the synthesis and electrochemical properties of redox active colloids incorporating redox molecules such as viologens and organometallic ferrocene as pendants into inactive polymer colloids. These redox active colloids were used as anolyte and catholyte in a pRFB with 0.1 M $LiBF_4$ in acetonitrile electrolyte and commercial Celgard membrane [117]. When tested at very low current densities (C/20) this battery exhibited a voltage of 0.9 V with the coulombic and en-

ergy efficiencies higher than 90% during 10 charge/discharge cycles. However, despite the low concentration of the active colloid (10 mM), only 20% of the theoretical capacity was accessed probably due to limited electric transport and sedimentation issues in the ferrocene-based electrolyte.

In 2019, Nishide et al. showed a polymer-based RFB comprising redox-active nanoparticle dispersions with active-material concentrations as high as 1.5 M in aqueous sodium chloride solution, thus exceeding the limitation of the solubility of the corresponding monomers [118]. Redox flow cells were fabricated using TEMPO-polymer nanoparticles as active material in the positive compartment and either viologen-, or diazaanthraquinone substituted polymer nanoparticles as active material is the negative compartment (see Table 6). These neutral aqueous pRFBs exhibited voltages of 1.1 V to 1.3 V, practical charge capacities of 7.2 Ah/L (65% capacity utilization) and 6 Ah/L (15% capacity utilization), for viologen or anthraquinone-based polymers respectively. Almost simultaneously, Yan et al. also reported aqueous pRFB using particulate slurry electrolytes with multi-electron redox capability and fast charge transfer in acidic electrolytes [108]. In that work, poly(imides)-based slurries and poly(hydroquinone) concentrated slurries (1.0 M) were prepared in 2 M H_2SO_4 and tested in a batteries using size-exclusion dialysis membranes (see Bottom-right Fig. 14). The battery exhibited discharge capacity of 4.95 Ah/L under current density of 20 mA/cm^2 and discharge capacity retention of 70% after 300 cycles although the sloppy discharge profile and the relatively low voltage output (0.5 V) limited the energy density (see Table 6).

Conclusions and perspectives

All-polymer batteries are attracting a lot of interest over the last years as promising low cost and environmentally friendly energy storage solutions. The inherent features of redox polymers such as processability, biobased & recyclability, and high rate performance make them very attractive for next generation battery technologies. In this review, a comprehensive summary of the various organic battery prototypes such as all-polymer batteries, polymer-air batteries and polymer redox-flow batteries have been discussed. Despite tremendous efforts, the development of just polymer battery technology is still at an early stage, and several challenges still need to be overcome before becoming a commercial reality.

From a materials perspective, the search for redox polymers with either ultralow or ultra-high redox potential, higher specific capacities (i.e. $>$ 200 mAh.g^{-1}) and long-term cycling stability (i.e. $>$ 85% capacity retention for 1 K cycles) is an on-going task. In particular, new polymers with low redox potential to be used as anode materials are less abundant and versatile than the current redox polymer cathode tool box. Additionally, the perspective to design novel redox polymers from renewable resources (biobased) is also a very attractive prospect for the development of more sustainable energy storage devices. Other alternatives, such as biodegradable redox polymers or redox polymers coming from recycled materials using a circular economy approaches, will have an important role in the future developments[119]. Future progress in the aforementioned research aspects, along with the development of cheap manufacturing techniques adapted to redox polymer such as 2D/3D printing and roll-to-roll processing, will enable all-polymer batteries to become a commercial reality in the future.

From a device perspective there are several aspects to be improved in both static and flow batteries. For static batteries, its energy storage capacity needs to be improved by developing devices, which deliver high potential ($>$3 V) and superior stability and cyclability. Here, besides the redox polymers, the development of electrolytes and device engineering is of a crucial importance. Indeed, the electrochemical performance of a redox polymer is highly dependent on the type of supporting electrolyte used (i.e. salt and solvent), which make the development of an all-polymer battery challenging since electrolyte needs to be optimized for both redox polymer electrodes [86,90]. Moreover, the development of supporting electrolyte to suit specific battery operation requirements (i.e. ultralow battery operating temperature, $<$ 0 °C) is also important aspect of the development of all-polymer batteries. Furthermore, electrode engineering represents a crucial optimisation step in order to develop redox polymer electrodes with practical areal capacity, and thus becoming a commercial reality [120]. Indeed, low areal capacity electrodes are generally employed in the literature of redox polymer for energy storage application, ranging from 0.1 to 0.3 mAh.cm^{-2}, as high content of carbon additive is needed to ensure sufficient electronic conductivity within the electrode to enable high-rate permanence and full active material utilization. This is in sharp contrast with the electrode criteria for commercial lithium-ion batteries, where electrodes with areal capacity superior than that of 2 mAh.cm^{-2} is generally achieved [121,122]. Recent works from both Nishide and co-workers[84] and Marcilla and co-workers [99], gave insights on some new electrode engineering concepts and formulation methods for redox polymers, through the use of single-walled carbon nanotubes, enabling redox polymer electrode with areal capacity up to 6.4 mAh.cm^{-2}.

On the other hand, the development of dynamic polymer redox flow batteries also needs to address several challenges. Beside the progress on macromolecular engineering to achieve highly soluble polymers with high specific capacity and adequate redox potential, the most important drawback of this technology is the high viscosity of both polymer solutions (in those few cases where high concentration is achieved) and specially of semisolid particulated dispersions. This fact provokes an increase in the pumping cost of the electrolyte and rate kinetic limitations due to high transport resistance of the electrolyte, being the main reason of the low power densities achieved by pRFB to date. Moreover, the presence of polymer particles and agglomerates might cause the clogging of current collectors commonly used in flow batteries which are based on porous carbons (eg. carbon felt, carbon paper) which results in a premature failure of the battery. A proper analysis of rheological properties of these electrolytes and the development of strategies to reduce the viscosity of such electrolytes are needed. The proper design of current collectors with more open 3D structures will be also necessary to bring polymer redox flow batteries closer to practical applications. Addressing these challenges should hold a bright future for organic batteries based on redox polymers given the development of the internet of things and mobile devices, where low-cost, sustainable, lightweight and flexible energy storage systems are desired.

Credit author statement

All authors contributed equally in the discussions and writing process.

Declaration of Competing Interest

There is no conflict of interest to be considered

Acknowledgment

Authors thank POLYSTORAGE ETN project, this project has received funding from the European Union's Horizon 2020 research and innovation programme under the Marie Skłodowska-Curie grant agreement No 860403. RM and NP thank the Spanish MCI through the SUSBAT project (Ref. RTI2018–101049-B-I00) and Juan de la Cierva fellowship [FJC2018–037781-I] (MCI-AEI/FEDER, UE). NC would like to thank the University of the Basque Country for

funding through a specialization of research staff fellowship (ES-PDOC 19/99). NG acknowledges the funding from the European Union's Horizon 2020 framework programme under the Marie Skłodowska-Curie Agreement No. 101028682.

Supplementary materials

Supplementary material associated with this article can be found, in the online version, at doi:10.1016/j.progpolymsci.2021.101449.

References

[1] Poizot P, Gaubicher J, Renault S, Dubois L, Liang Y, Yao Y. Opportunities and challenges for organic electrodes in electrochemical energy storage. Chem Rev 2020;120:6490–557. doi:10.1021/acs.chemrev.9b00482.
[2] Tran MK, Rodrigues MTF, Kato K, Babu G, Ajayan PM. Deep eutectic solvents for cathode recycling of Li-ion batteries. Nat Energy 2019;4:339–45. doi:10.1038/s41560-019-0368-4.
[3] Song Z, Zhou H. Towards sustainable and versatile energy storage devices: an overview of organic electrode materials. Energy Environ Sci 2013;6:2280–301. doi:10.1039/c3ee40709h.
[4] Häupler B, Wild A, Schubert US. Carbonyls: powerful organic materials for secondary batteries. Adv Energy Mater 2015;5:1402034. doi:10.1002/aenm.201402034.
[5] Williams DL, Byrne JJ, Driscoll JS. A high energy density lithium/dichloroisocyanuric acid battery system. J Electrochem Soc 1969;116:2. doi:10.1149/1.2411755.
[6] Alt H, Binder H, Köhling A, Sandstede G. Investigation into the use of quinone compounds-for battery cathodes. Electrochim Acta 1972;17:873–87. doi:10.1016/0013-4686(72)90010-2.
[7] Goto F, Abe K, Ikabayashi K, Yoshida T, Morimoto H. The polyaniline/lithium battery. J Power Sources 1987;20:243–8. doi:10.1016/0378-7753(87)80118-0.
[8] Matsunaga T, Daifuku H, Kawagoe T. Development of polyaniline-iithium secondary battery. Nippon Kagaku Kaishi 1990;1990:1–11. doi:10.1246/nikkashi.1990.1.
[9] Yoshino A. The birth of the lithium-ion battery. Angew Chem Int Ed 2012;51:5798–800. doi:10.1002/anie.201105006.
[10] Zhang H, Li C, Eshetu GG, Laruelle S, Grugeon S, Zaghib K, et al. From solid-solution electrodes and the rocking-chair concept to today's batteries. Angew Chem Int Ed 2020;59:534–8. doi:10.1002/anie.201913923.
[11] Muench S, Wild A, Friebe C, Häupler B, Janoschka T, Schubert US. Polymer-based organic batteries. Chem Rev 2016;116:9438–84. doi:10.1021/acs.chemrev.6b00070.
[12] Sun T, Xie J, Guo W, Li DS, Zhang Q. Covalent-organic frameworks: advanced organic electrode materials for rechargeable batteries. Adv Energy Mater 2020;1904199:1904199. doi:10.1002/aenm.201904199.
[13] Poizot P, Dolhem F, Gaubicher J. Progress in all-organic rechargeable batteries using cationic and anionic configurations: toward low-cost and greener storage solutions? Curr Opin Electrochem 2018;9:70–80. doi:10.1016/j.coelec.2018.04.003.
[14] Friebe C, Lex-Balducci A, Schubert US. Sustainable energy storage: recent trends and developments toward fully organic batteries. ChemSusChem 2019;12:4093–115. doi:10.1002/cssc.201901545.
[15] Esser B. Redox polymers as electrode-active materials for batteries. Org Mater 2019;01:063–70. doi:10.1055/s-0039-3401016.
[16] Bénière F, Boils D, Cánepa H, Franco J, Le Corre A, Louboutin JP. Solid state batteries with conducting polymers. Le J Phys Colloq 1983;44 C3-567-C3-572. doi:10.1051/jphyscol:19833112.
[17] Okuzaki H, Suzuki H, Ito T. Electromechanical Properties of Poly(3,4-ethylenedioxythiophene)/Poly(4-styrene sulfonate) Films. J Phys Chem B 2009;113:11378–83. doi:10.1021/jp902845x.
[18] Zhao Z, Richardson GF, Meng Q, Zhu S, Kuan HC, Ma J. PEDOT-based composites as electrode materials for supercapacitors. Nanotechnology 2015;27. doi:10.1088/0957-4484/27/4/042001.
[19] Nakahara K, Oyaizu K, Nishide H. Organic radical battery approaching practical use. Chem Lett 2011;40:222–7. doi:10.1246/cl.2011.222.
[20] Suga T, Ohshiro H, Sugita S, Oyaizu K, Nishide H, Ugita S, et al. Emerging N-type redox-active radical polymer for a totally organic polymer-based rechargeable battery. Adv Mater 2009;21:1627–30. doi:10.1002/adma.200803073.
[21] Miyasaka M, Yamazaki T, Tsuchida E, Nishide H. Regioregular polythiophenl with pendant phenoxyl radicals: a new high-spin organic polymer. Macromolecules 2000;33:8211–17. doi:10.1021/ma000993l.
[22] Jähnert T, Hager MD, Schubert US. Assorted phenoxyl-radical polymers and their application in lithium-organic batteries. Macromol Rapid Commun 2016;37:725–30. doi:10.1002/marc.201500702.
[23] Friebe C, Schubert US. High-power-density organic radical batteries. Top Curr Chem 2017;375:1–35. doi:10.1007/s41061-017-0103-1.
[24] Yokoji T, Kameyama Y, Maruyama N, Matsubara H. High-capacity organic cathode active materials of 2,2′-bis-p-benzoquinone derivatives for rechargeable batteries. J Mater Chem A 2016;4:5457–66. doi:10.1039/C5TA10713J.
[25] Hernández G, Lago N, Shanmukaraj D, Armand M, Mecerreyes D. Polyimide-polyether binders–diminishing the carbon content in lithium[*sbnd*]sulfur batteries. Mater Today Energy 2017;6:264–70. doi:10.1016/j.mtener.2017.11.001.
[26] Banda H, Damien D, Nagarajan K, Hariharan M, Shaijumon MM. A polyimide based all-organic sodium ion battery. J Mater Chem A 2015;3:10453–8. doi:10.1039/c5ta02043c.
[27] Hernández G, Salsamendi M, Morozova SM, Lozinskaya EI, Devaraj S, Vygodskii YS, et al. Polyimides as cathodic materials in lithium batteries: effect of the chemical structure of the diamine monomer. J Polym Sci Part A Polym Chem 2018;56:714–23. doi:10.1002/pola.28937.
[28] Wild A, Strumpf M, Häupler B, Hager MD, Schubert US. All-organic battery composed of thianthrene- and TCAQ-based polymers. Adv Energy Mater 2017;7:1601415. doi:10.1002/aenm.201601415.
[29] Dong X, Yu H, Ma Y, Bao JL, Truhlar DG, Wang Y, et al. All-organic rechargeable battery with reversibility supported by "water-in-salt" electrolyte. Chem A Eur J 2017;23:2560–5. doi:10.1002/chem.201700063.
[30] Sano N, Tomita W, Hara S, Min C-M, Lee JS, Oyaizu K, et al. Polyviologen hydrogel with high-rate capability for anodes toward an aqueous electrolyte-type and organic-based rechargeable device. ACS Appl Mater Interfaces 2013;5:1355–61. doi:10.1021/am302647w.
[31] Gomez I, Leonet O, Blazquez JA, Mecerreyes D. Inverse vulcanization of sulfur using natural dienes as sustainable materials for lithium-sulfur batteries. ChemSusChem 2016;9:3419–25. doi:10.1002/cssc.201601474.
[32] Pirnat K, Casado N, Porcarelli L, Ballard N, Mecerreyes D. Synthesis of redox polymer nanoparticles based on poly(vinyl catechols) and their electroactivity. Macromolecules 2019;52:8155–66. doi:10.1021/acs.macromol.9b01405.
[33] Li J, Jing X, Li Q, Li S, Gao X, Feng X, et al. Bulk COFs and COF nanosheets for electrochemical energy storage and conversion. Chem Soc Rev 2020;49:3565–604. doi:10.1039/d0cs00017e.
[34] Molina A, Patil N, Ventosa E, Liras M, Palma J, Marcilla R. New anthraquinone-based conjugated microporous polymer cathode with ultrahigh specific surface area for high-performance lithium-ion batteries. Adv Funct Mater 2019;1908074:1–11. doi:10.1002/adfm.201908074.
[35] Suga T, Sugita S, Ohshiro H, Oyaizu K, Nishide H. p- and n-type bipolar redox-active radical polymer: toward totally organic polymer-based rechargeable devices with variable configuration. Adv Mater 2011;23:751–4. doi:10.1002/adma.201003525.
[36] MacInnes D, Druy MA, Nigrey PJ, Nairns DP, MacDiarmid AG, Heeger AJ. Organic batteries: reversible n- and p- type electrochemical doping of polyacetylene, (CH) x. J Chem Soc Chem Commun 1981:317–19. doi:10.1039/c39810000317.
[37] Chiang CK. An all-polymeric solid state battery. Polymer (Guildf) 1981;22:1454–6. doi:10.1016/0032-3861(81)90309-8.
[38] Walatka VV, Labes MM, Perlstein JH. Polysulfur nitride-a one-dimensional chain with a metallic ground state. Phys Rev Lett 1973;31:1139–42. doi:10.1103/PhysRevLett.31.1139.
[39] Greene RL, Street GB, Suter LJ. Superconductivity in polysulfur nitride (SN) X. Phys Rev Lett 1975;34:577–9. doi:10.1017/CBO9781107415324.004.
[40] Shirakawa H, Louis EJ, MacDiarmid AG, Chiang CK, Heeger AJ. Synthesis of electrically conducting organic polymers: halogen derivatives of polyacetylene, (CH)x. J Chem Soc Chem Commun 1977:578–80. doi:10.1039/C39770000578.
[41] Chiang CK, Park YW, Heeger AJ, Shirakawa H, Louis EJ, MacDiarmid AG. Conducting polymers: halogen doped polyacetylene. J Chem Phys 1978;69:5098–104. doi:10.1063/1.436503.
[42] Audenaert M, Gusman G, Deltour R. Electrical conductivity of in doped polyacetylene. Phys Rev B 1981;24:7380–2. doi:10.1103/PhysRevB.24.7380.
[43] Bredas JL, Street GB. Polarons, bipolarons, and solitons in conducting polymers. Acc Chem Res 1985;18:309–15. doi:10.1021/ar00118a005.
[44] Cai Z, Geng M, Tang Z. Novel battery using conducting polymers: polyindole and polyaniline as active materials. J Mater Sci 2004;39:4001–3. doi:10.1023/B:JMSC.0000031481.12810.39.
[45] Zhu LM, Lei AW, Cao YL, Ai XP, Yang HX. An all-organic rechargeable battery using bipolar polyparaphenylene as a redox-active cathode and anode. Chem Commun 2013;49:567–9. doi:10.1039/C2CC36622C.
[46] Nyström G, Razaq A, Strømme M, Nyholm L, Mihranyan A. Ultrafast all-polymer paper-based batteries. Nano Lett 2009;9:3635–9. doi:10.1021/nl901852h.
[47] Zhu LM, Shi W, Zhao RR, Cao YL, Ai XP, Lei AW, et al. n-Dopable polythiophenes as high capacity anode materials for all-organic Li-ion batteries. J Electroanal Chem 2013;688:118–22. doi:10.1016/j.jelechem.2012.06.019.
[48] De Surville R, Jozefowicz M, Yu LT, Pepichon J, Buvet R. Electrochemical chains using protolytic organic semiconductors. Electrochim Acta 1968;13:1451–8. doi:10.1016/0013-4686(68)80071-4.
[49] Kaneto K, Yoshino K, Inuishi Y. Characteristics of Polythiophene Battery. Jpn J Appl Phys 1983;22:L567–8. doi:10.1143/JJAP.22.L567.
[50] Killian JG, Coffey BM, Gao F, Poehler TO, Searson PC. Polypyrrole composite electrodes in an all-polymer battery system. J Electrochem Soc 1996;143:936. doi:10.1149/1.1836562.
[51] Wang CY, Ballantyne AM, Hall SB, Too CO, Officer DL, Wallace GG. Functionalized polythiophene-coated textile: a new anode material for a flexible battery. J Power Sources 2006;156:610–14. doi:10.1016/j.jpowsour.2005.06.020.
[52] Sultana I, Rahman MM, Wang J, Wang C, Wallace GG, Liu HK. All-polymer battery system based on polypyrrole (PPy)/para (toluene sulfonic acid) (pTS) and polypyrrole (PPy)/indigo carmine (IC) free standing films. Electrochim Acta 2012;83:209–15. doi:10.1016/j.electacta.2012.08.043.

[53] Zhijiang C. Study on a novel polymer-based secondary battery system. J Polym Res 2006;13:207–11. doi:10.1007/s10965-005-9027-5.
[54] Lee JY, Ong LH, Chuah GK. Rechargeable thin film batteries of polypyrrole and polyaniline. J Appl Electrochem 1992;22:738–42. doi:10.1007/BF01027503.
[55] Wang CY, Tsekouras G, Wagner P, Gambhir S, Too CO, Officer D, et al. Functionalised polyterthiophenes as anode materials in polymer/polymer batteries. Synth Met 2010;160:76–82. doi:10.1016/j.synthmet.2009.10.001.
[56] Xuan Y, Sandberg M, Berggren M, Crispin X. An all-polymer-air PEDOT battery. Org Electron 2012;13:632–7. doi:10.1016/j.orgel.2011.12.018.
[57] Reyes-Reyes M, López-Sandoval R. Optimizing the oxidation level of PEDOT anode in air-PEDOT battery. Org Electron 2018;52:364–70. doi:10.1016/j.orgel.2017.11.016.
[58] Moia D, Giovannitti A, Szumska AA, Maria IP, Rezasoltani E, Sachs M, et al. Design and evaluation of conjugated polymers with polar side chains as electrode materials for electrochemical energy storage in aqueous electrolytes. Energy Environ Sci 2019;12:1349–57. doi:10.1039/c8ee03518k.
[59] Deng W, Liang X, Wu X, Qian J, Cao Y, Ai X, et al. A low cost, all-organic Na-ion battery based on polymeric cathode and anode. Sci Rep 2013;3:2671. doi:10.1038/srep02671.
[60] Emanuelsson R, Sterby M, Strømme M, Sjödin M. An all-organic proton battery. J Am Chem Soc 2017;139:4828–34. doi:10.1021/jacs.7b00159.
[61] Xie J, Wang Z, Xu ZJ, Zhang Q. Toward a high-performance all-plastic full battery with a'Single organic polymer as both cathode and anode. Adv Energy Mater 2018;8:1703509. doi:10.1002/aenm.201703509.
[62] Hernández G, Casado N, Zamarayeva AM, Duey JK, Armand M, Arias AC, et al. Perylene polyimide-polyether anodes for aqueous all-organic polymer batteries. ACS Appl Energy Mater 2018;1:7199–205. doi:10.1021/acsaem.8b01663.
[63] Qin J, Lan Q, Liu N, Men F, Wang X, Song Z, et al. A metal-free battery with pure ionic liquid electrolyte. iScience 2019;15:16–27. doi:10.1016/j.isci.2019.04.010.
[64] Emanuelsson R, Karlsson C, Huang H, Kosgei C, Strømme M, Sjödin M. Quinone based conducting redox polymers for electrical energy storage. Russ J Electrochem 2017;53:8–15. doi:10.1134/S1023193517010050.
[65] Senoh H, Yao M, Sakaebe H, Yasuda K, Siroma Z. A two-compartment cell for using soluble benzoquinone derivatives as active materials in lithium secondary batteries. Electrochim Acta 2011;56:10145–50. doi:10.1016/j.electacta.2011.08.115.
[66] Emanuelsson R, Huang H, Gogoll A, Strømme M, Sjödin M. Enthalpic versus entropic contribution to the quinone formal potential in a polypyrrole-based conducting redox polymer. J Phys Chem C 2016;120:21178–83. doi:10.1021/acs.jpcc.6b05353.
[67] Åkerlund L, Emanuelsson R, Renault S, Huang H, Brandell D, Strømme M, et al. The proton trap technology-toward high potential quinone-based organic energy storage. Adv Energy Mater 2017;7:1700259. doi:10.1002/aenm.201700259.
[68] Åkerlund L, Emanuelsson R, Hernández G, Ruipérez F, Casado N, Brandell D, et al. In situ investigations of a proton trap material: a PEDOT-based copolymer with hydroquinone and pyridine side groups having robust cyclability in organic electrolytes and ionic liquids. ACS Appl Energy Mater 2019;2:4486–95. doi:10.1021/acsaem.9b00735.
[69] Karlsson C, Strietzel C, Huang H, Sjödin M, Jannasch P. Nonstoichiometric triazolium protic ionic liquids for all-organic batteries. ACS Appl Energy Mater 2018;1:6451–62. doi:10.1021/acsaem.8b01389.
[70] Zhu X, Zhao R, Deng W, Ai X, Yang H, Cao Y. An all-solid-state and all-organic sodium-ion battery based on redox-active polymers and plastic crystal electrolyte. Electrochim Acta 2015;178:55–9. doi:10.1016/j.electacta.2015.07.163.
[71] Ajjan FN, Casado N, Rębiś T, Elfwing A, Solin N, Mecerreyes D, et al. High performance PEDOT/lignin biopolymer composites for electrochemical supercapacitors. J Mater Chem A 2016;4:1838–47. doi:10.1039/c5ta10096h.
[72] Casado N, Hilder M, Pozo-Gonzalo C, Forsyth M, Mecerreyes D. Electrochemical behavior of PEDOT/lignin in ionic liquid electrolytes: suitable cathode/electrolyte system for sodium batteries. ChemSusChem 2017;10:1783–91. doi:10.1002/cssc.201700012.
[73] Patil N, Mavrandonakis A, Jérôme C, Detrembleur C, Casado N, Mecerreyes D, et al. High-performance all-organic aqueous batteries based on a poly(imide) anode and poly(catechol) cathode. J Mater Chem A 2021. doi:10.1039/D0TA09404H.
[74] Song Z, Zhan H, Zhou Y. Polyimides: promising energy-storage materials. Angew Chem Int Ed 2010;49:8444–8. doi:10.1002/anie.201002439.
[75] Zhang Y, An Y, Yin B, Jiang J, Dong S, Dou H, et al. A novel aqueous ammonium dual-ion battery based on organic polymers. J Mater Chem A 2019;7:11314–20. doi:10.1039/C9TA00254E.
[76] Nakahara K, Iwasa S, Satoh M, Morioka Y, Iriyama J, Suguro M, et al. Rechargeable batteries with organic radical cathodes. Chem Phys Lett 2002;359:351–4. doi:10.1016/S0009-2614(02)00705-4.
[77] Hernández G, Casado N, Coste R, Shanmukaraj D, Rubatat L, Armand M, et al. Redox-active polyimide–polyether block copolymers as electrode materials for lithium batteries. RSC Adv 2015;5:17096–103. doi:10.1039/C4RA15976D.
[78] Dong X, Guo ZZ, Guo ZZ, Wang Y, Xia Y. Organic batteries operated at −70°C. Joule 2018;2:902–13. doi:10.1016/j.joule.2018.01.017.
[79] Qin J, Lan Q, Liu N, Zhao Y, Song Z, Zhan H. A metal-free battery working at −80°C. Energy Storage Mater 2020;26:585–92. doi:10.1016/j.ensm.2019.12.002.
[80] Zhou G, An X, Zhou C, Wu Y, Miao Y-E, Liu T. Highly porous electroactive polyimide-based nanofibrous composite anode for all-organic aqueous ammonium dual-ion batteries. Compos Commun 2020;22:100519. doi:10.1016/j.coco.2020.100519.
[81] Strietzel C, Sterby M, Huang H, Strømme M, Emanuelsson R, Sjödin M. An aqueous conducting redox-polymer-based proton battery that can withstand rapid constant-voltage charging and sub-zero temperatures. Angew Chem. 2020;132:9718–25. doi:10.1002/ange.202001191.
[82] Suga T, Pu YJ, Kasatori S, Nishide H. Cathode- and anode-active poly(nitroxylstyrene)s for rechargeable batteries: P- and n-type redox switching via substituent effects. Macromolecules 2007;40:3167–73. doi:10.1021/ma0628578.
[83] Koshika K, Chikushi N, Sano N, Oyaizu K, Nishide H. A TEMPO-substituted polyacrylamide as a new cathode material: an organic rechargeable device composed of polymer electrodes and aqueous electrolyte. Green Chem 2010;12:1573–5. doi:10.1039/b926296b.
[84] Hatakeyama-Sato K, Wakamatsu H, Katagiri R, Oyaizu K, Nishide H. An ultrahigh output rechargeable electrode of a hydrophilic radical polymer/nanocarbon hybrid with an exceptionally large current density beyond 1 Acm^{-2}. Adv Mater 2018;30:1–6. doi:10.1002/adma.201800900.
[85] Chikushi N, Yamada H, Oyaizu K, Nishide H. TEMPO-substituted polyacrylamide for an aqueous electrolyte-typed and organic-based rechargeable device. Sci China Chem 2012;55:822–9. doi:10.1007/s11426-012-4556-3.
[86] Jähnert T, Häupler B, Janoschka T, Hager MD, Schubert US. Synthesis and charge-discharge studies of poly(ethynylphenyl)galvinoxyles and their use in organic radical batteries with aqueous electrolytes. Macromol Chem Phys 2013;214:2616–23. doi:10.1002/macp.201300408.
[87] Hatakeyama-Sato K, Wakamatsu H, Yamagishi K, Fujie T, Takeoka S, Oyaizu K, et al. Ultrathin and stretchable rechargeable devices with organic polymer nanosheets conformable to skin surface. Small 2019;15:1805296. doi:10.1002/smll.201805296.
[88] Muench S, Burges R, Lex-Balducci A, Brendel JC, Jäger M, Friebe C, et al. Printable ionic liquid-based gel polymer electrolytes for solid state all-organic batteries. Energy Storage Mater 2020;25:750–5. doi:10.1016/j.ensm.2019.09.011.
[89] Hatakeyama-Sato K, Tezuka T, Ichinoi R, Matsumono S, Sadakuni K, Oyaizu K. Metal-free, solid-state, paperlike rechargeable batteries consisting of redox-active polyethers. ChemSusChem 2020;13:2443–8. doi:10.1002/cssc.201903175.
[90] Oka K, Kato R, Oyaizu K, Nishide H. Poly(vinyldibenzothiophenesulfone): its redox capability at very negative potential toward an all-organic rechargeable device with high-energy density. Adv Funct Mater 2018;28:1805858. doi:10.1002/adfm.201805858.
[91] Casado N., Mantione D., Shanmukaraj D., Mecerreyes D. Symmetric all-organic battery containing a dual redox-active polymer as cathode and anode material. ChemSusChem 2019. 10.1002/cssc.201902856.
[92] Sen S, Saraidaridis J, Kim SY, Palmore GTR. Viologens as charge carriers in a polymer-based battery anode. ACS Appl Mater Interfaces 2013;5:7825–30. doi:10.1021/am401590q.
[93] Yao M, Sano H, Ando H, Kiyobayashi T. Molecular ion battery: a rechargeable system without using any elemental ions as a charge carrier. Sci Rep 2015;5:1–8. doi:10.1038/srep10962.
[94] Suo L, Borodin O, Gao T, Olguin M, Ho J, Fan X, et al. Water-in-salt" electrolyte enables high-voltage aqueous lithium-ion chemistries. Science (80-) 2015;350:938–43. doi:10.1126/science.aab1595.
[95] Chawla N. Recent advances in air-battery chemistries. Mater Today Chem 2019;12:324–31. doi:10.1016/j.mtchem.2019.03.006.
[96] Imanishi N, Yamamoto O. Perspectives and challenges of rechargeable lithium–air batteries. Mater Today Adv 2019;4:100031. doi:10.1016/j.mtadv.2019.100031.
[97] Zhang J, Zhou Q, Tang Y, Zhang L, Li Y. Zinc-air batteries: are they ready for prime time? Chem Sci 2019;10:8924–9. doi:10.1039/c9sc04221k.
[98] Choi W, Harada D, Oyaizu K, Nishide H. Aqueous electrochemistry of poly(vinylanthraquinone) for anode-active materials in high-density and rechargeable polymer/air batteries. J Am Chem Soc 2011;133:19839–43. doi:10.1021/ja206961t.
[99] Molina A, Patil N, Ventosa E, Liras M, Palma J, Marcilla R. Electrode engineering of redox-active conjugated microporous polymers for ultra-high areal capacity organic batteries. ACS Energy Lett 2020;5:2945–53. doi:10.1021/acsenergylett.0c01577.
[100] Kawai T, Oyaizu K, Nishide H. High-density and robust charge storage with poly(anthraquinone-substituted norbornene) for organic electrode-active materials in polymer–air secondary batteries. Macromolecules 2015;48:2429–34. doi:10.1021/ma502396r.
[101] Li Y, Liu L, Liu C, Lu Y, Shi R, Li F, et al. Rechargeable aqueous polymer-air batteries based on polyanthraquinone anode. Chem 2019;5:2159–70. doi:10.1016/j.chempr.2019.06.001.
[102] Oka K, Strietzel C, Emanuelsson R, Nishide H, Oyaizu K, Strømme M, et al. Conducting redox polymer as a robust organic electrode-active material in acidic aqueous electrolyte towards polymer–air secondary batteries. ChemSusChem 2020;13:2280–5. doi:10.1002/cssc.202000627.
[103] Oka K, Murao S, Kobayashi K, Nishide H, Oyaizu K. Charge- and proton-storage capability of naphthoquinone-substituted poly(allylamine) as electrode-active material for polymer-air secondary batteries. ACS Appl Energy Mater 2020. doi:10.1021/acsaem.0c02178.
[104] Lai YY, Li X, Zhu Y. Polymeric active materials for redox flow battery application. ACS Appl Polym Mater 2020;2:113–28. doi:10.1021/acsapm.9b00864.

[105] Janoschka T, Martin N, Martin U, Friebe C, Morgenstern S, Hiller H, et al. An aqueous, polymer-based redox-flow battery using non-corrosive, safe, and low-cost materials. Nature 2015;527:78–81. doi:10.1038/nature15746.
[106] Winsberg J, Benndorf S, Wild A, Hager MD, Schubert US. Synthesis and characterization of a phthalimide-containing redox-active polymer for high-voltage polymer-based redox-flow batteries. Macromol Chem Phys 2018;219:1–7. doi:10.1002/macp.201700267.
[107] Winsberg J, Hagemann T, Muench S, Friebe C, Häupler B, Janoschka T, et al. Poly(boron-dipyrromethene)—a redox-active polymer class for polymer redox-flow batteries. Chem Mater 2016;28:3401–5. doi:10.1021/acs.chemmater.6b00640.
[108] Yan W, Wang C, Tian J, Zhu G, Ma L, Wang Y, et al. All-polymer particulate slurry batteries. Nat Commun 2019;10:2513. doi:10.1038/s41467-019-10607-0.
[109] Winsberg J, Janoschka T, Morgenstern S, Hagemann T, Muench S, Hauffman G, et al. Poly(TEMPO)/Zinc hybrid-flow battery: a novel, "green," high voltage, and safe energy storage system. Adv Mater 2016;28:2238–43. doi:10.1002/adma.201505000.
[110] Hagemann T, Strumpf M, Schröter E, Stolze C, Grube M, Nischang I, et al. (2,2,6,6-Tetramethylpiperidin-1-yl)oxyl-containing zwitterionic polymer as catholyte species for high-capacity aqueous polymer redox flow batteries. Chem Mater 2019;31:7987–99. doi:10.1021/acs.chemmater.9b02201.
[111] Nagarjuna G, Hui J, Cheng KJ, Lichtenstein T, Shen M, Moore JS, et al. Impact of redox-active polymer molecular weight on the electrochemical properties and transport across porous separators in nonaqueous solvents. J Am Chem Soc 2014;136:16309–16. doi:10.1021/ja508482e.
[112] Burgess M, Chénard E, Hernández-Burgos K, Nagarjuna G, Assary RS, Hui J, et al. Impact of backbone tether length and structure on the electrochemical performance of viologen redox active polymers. Chem Mater 2016;28:7362–74. doi:10.1021/acs.chemmater.6b02825.
[113] Montoto EC, Nagarjuna G, Moore JS, Rodríguez-López J. Redox active polymers for non-aqueous redox flow batteries: validation of the size-exclusion approach. J Electrochem Soc 2017;164:A1688–94. doi:10.1149/2.1511707jes.
[114] Montoto EC, Cao Y, Hernández-Burgos K, Sevov CS, Braten MN, Helms BA, et al. Effect of the backbone tether on the electrochemical properties of soluble cyclopropenium redox-active polymers. Macromolecules 2018;51:3539–46. doi:10.1021/acs.macromol.8b00574.
[115] Sukegawa T, Masuko I, Oyaizu K, Nishide H. Expanding the dimensionality of polymers populated with organic robust radicals toward flow cell application: synthesis of TEMPO-crowded bottlebrush polymers using anionic polymerization and ROMP. Macromolecules 2014;47:8611–17. doi:10.1021/ma501632t.
[116] Oh SH, Lee CW, Chun DH, Jeon JD, Shim J, Shin KH, et al. A metal-free and all-organic redox flow battery with polythiophene as the electroactive species. J Mater Chem A 2014;2:19994–8. doi:10.1039/c4ta04730c.
[117] Montoto EC, Nagarjuna G, Hui J, Burgess M, Sekerak NM, Hernández-Burgos K, et al. Redox active colloids as discrete energy storage carriers. J Am Chem Soc 2016;138:13230–7. doi:10.1021/jacs.6b06365.
[118] Hatakeyama-Sato K, Nagano T, Noguchi S, Sugai Y, Du J, Nishide H, et al. Hydrophilic organic redox-active polymer nanoparticles for higher energy density flow batteries. ACS Appl Polym Mater 2019;1:188–96. doi:10.1021/acsapm.8b00074.
[119] Ajjan FN, Mecerreyes D, Inganäs O. Enhancing energy storage devices with biomacromolecules in hybrid electrodes. Biotechnol J 2019;14:1–10. doi:10.1002/biot.201900062.
[120] Kim J, Kim JH, Ariga K. Redox-active polymers for energy storage nanoarchitectonics. Joule 2017;1:739–68. doi:10.1016/j.joule.2017.08.018.
[121] Zhu K, Li Q, Xue Z, Yu Q, Liu X, Shan Z, et al. Mesoporous TiO_2 spheres as advanced anodes for low-cost, safe, and high-areal-capacity lithium-ion full batteries. ACS Appl Nano Mater 2020;3:1019–27. doi:10.1021/acsanm.9b02594.
[122] Park SH, King PJ, Tian R, Boland CS, Coelho J, Zhang C, et al. High areal capacity battery electrodes enabled by segregated nanotube networks. Nat Energy 2019;4:560–7. doi:10.1038/s41560-019-0398-y.